Supplementary Information for

Reversible conformational change coupled electron transfer (CCET) for stable redox-active molecules

An Kitamura, Jake M. Evans, Christian A. Malapit*

Department of Chemistry, Northwestern University, Technological Institute, Evanston, Illinois 60208, United States

*Correspondence to: christian.malapit@northwestern.edu

Table of Contents

Materials and Methods

General Information. Unless otherwise noted, all manipulations were carried out using standard Schlenk or glovebox techniques under a N_2 atmosphere. NMR spectra were obtained on a Bruker Avance 500 MHz spectrometer. ^1H chemical shifts are reported in ppm relative to trimethylsilane, with the residual solvent peak used as an internal reference.

Anhydrous solvents, acetonitrile (Fisher Scientific), dimethylformamide (Fisher Scientific), tetrahydrofuran (Fisher Scientific)) were passed through a Pure Process Technologies solvent purification system (SPS) before use. Solvents were brought into the glovebox directly from the SPS using a J Young round bottom flask.

Supporting electrolytes were purchased from the following vendors and dried under high vacuum for 48 h at 90-120 °C before being transferred to glovebox. Tetrabutylammonium hexafluorophosphate 98% ($TBAPF_6$), Lithium Bis(trifluoromethanesulfonyl)imide 98.0+% (LiTFSI) was obtained from Tokyo Chemical Industry America, Inc. Tetra-n-butylammonium tetrafluoroborate 99% ($TBABF_4$) and Potassium hexafluorophosphate 99% (KPF_6) was obtained from Thermo Scientific Chemicals.

Anolyte compounds were purchased from the following vendors, dried under high vacuum for 24 hours and transferred to the glovebox. Benzil 99%, 9,10-phenanthrenequinone (PQ) 99%, were obtained from Tokyo Chemical Industry America, Inc. Acenaphthylene-1,2-dione (ANQ) 95% and 2,2'-Thenil 98% were obtained from Thermo Scientific Chemicals. Furil 98% and 1,2-Di-3-thienyl-1,2-ethanedione (3,3'-Thenil) 98% were obtained from Combi-Blocks, Inc. Benzo[1,2-b:4,3-b']dithiophene-4,5-dione (2,2'-BDTP) 95% and Benzo[1,2-b:6,5-b']dithiophene-4,5-dione (4,4'-BDTP) 97% were obtained from Ambeed, Inc.

Solubility. Solubility in DMF was determined by mass measurements. A saturated solution of the compound was prepared in DMF. The solution was then filtered to remove any undissolved material, and an aliquot was dispensed into tared vials. The solvent was evaporated under high vacuum, and the vial containing the dried dissolved solid was re-weighed. The dissolved mass was determined from the difference between the tared vial and the new vial weight containing dried solid. The concentration of the compound was calculated using the dissolved mass and the volume of the solvent placed into the vial.

Electrochemistry Experimental Methods

Cyclic Voltammetry. Cyclic Voltammetry was performed in a nitrogen filled MBraun glovebox or in air with a nitrogen balloon purging the system. All measurements were recorded using a Biologic VSP multichannel potentiostat/galvanostat. A three-electrode set-up was employed, including a 3.0 mm diameter glassy carbon working electrode (BASi, MF-2012), a platinum wire as the counter and a silver/silver nitrate fritted reference electrode (BASi, MW-1085). The glassy carbon electrode was polished in between each data collection on a microcloth pad and when needed, more abrasive pads and 0.05 µm alumina were used (BASi, MF-2060). When this was done, working electrode was dried under vacuum before using to remove any residual water. 5 mM of ROM was used with an electrolyte concentration of 500 mM, scan rate was 400 mV/s unless stated otherwise. CVs were all reported as V vs. Fc/Fc^+.

Diffusion Coefficient Calculations. The diffusion coefficient was determined by employing the Randles-Sevcik method. CV's were taken at scan rates of 50 mV to 800 mV and the anodic and cathodic peak currents were recorded. These peak currents were then plotted vs. the square root of the scan rate which produced two linear relationships, one corresponding to reduction and the other the oxidation. Slopes were determined and used to calculate the diffusion coefficients based on the Randles-Sevcik Equation (Eq. 1).[1]

$$i_p = 0.4463 \times nFAC \times \sqrt{\frac{nF\nu D}{RT}} \quad \text{(Eq. 1)}$$

Equation terms: i_p is the peak current (A), n is the number of electrons transferred, F is Faraday's constant, A is the area of the electrode (cm^2), C is the concentration of redox active species (mol/cm^3), v is the scan rate (V/s), D is the diffusion coefficient (cm^2/s), R is the gas constant ($JK^{-1}\ mol^{-1}$), and T is the temperature (K).

Calculation of Electron Transfer Rate Constant. The Nicholson method was used to estimate the heterogenous electron transfer rate (Eq. 2-3).[2,3] Cyclic voltammetry were performed at scan rates of 50 mV to 800 mV and the difference of the anodic and cathodic peak potentials were recorded. The peak separation in mV was used to determine the dimensionless value, Ψ. k was then directly determined from the slope of the plot, Ψ vs. scan rate $v^{-1/2}$.

$$\Psi = \frac{(-0.6288+0.0021\times\Delta E_p)}{(1-0.017\times\Delta E_p)} \quad \text{(Eq. 2)}$$

$$\Psi = k \times \left(\frac{\pi DnFv}{RT}\right)^{-\frac{1}{2}} \quad \text{(Eq. 3)}$$

Equation terms: Ψ is the Nicholson dimensionless number, ΔE_p is the anodic and cathodic peak separation (V/s), k is the standard rate constant ($cm\ s^{-1}$), D is the diffusion coefficient (cm^2/s), n is the number of electrons transferred, F is Faraday's constant, v is the scan rate (V/s), R is the gas constant ($JK^{-1}\ mol^{-1}$), and T is the temperature (K).

	$E_{1/2}$	D_c	D_a	k_c	k_a	I_{pa}/I_{pc}
PQ	– 1.0	5.5	4.0	6.7	5.7	1.00
2,2'-BDTP	– 1.07	3.3	2.5	6.6	5.7	0.98
ANQ	– 1.29	5.2	3.7	3.9	3.3	0.97
4,4'-BDTP	– 1.38					
2,2'-thenil	– 1.31	2.7	1.8	9.8	7.9	0.99
Furil	– 1.40	4.2	3.2	7.9	6.9	0.95
Benzil	– 1.54	8.0	6.0	4.8	4.2	1.00
3,3'-thenil	– 1.55	7.8	5.2	9.9	8.1	0.97

Table S1. Half-wave potentials referenced against Fc/Fc^+ in 0.5 M $TBAPF_6$, DMF. Cathodic diffusion coefficient D_c (x 10^{-6} cm^2/s), anodic diffusion coefficient D_a (x 10^{-6} cm^2/s), cathodic electron transfer rate k_c (x 10^{-3} cm/s), and anodic electron transfer rates k_a (x 10^{-3} cm/s). The peak current ratios of the forward and reverse scan (I_{pa}/I_{pc}).

Cyclic Voltammograms

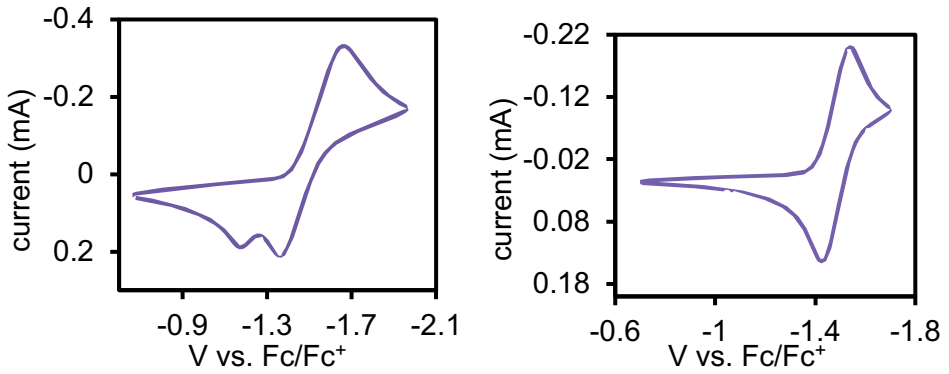

Figure S1. Cyclic voltammograms of 5 mM benzil in 0.5 M LiTFSI (left) and 0.25 M $TBABF_4$ (right) in DMF.

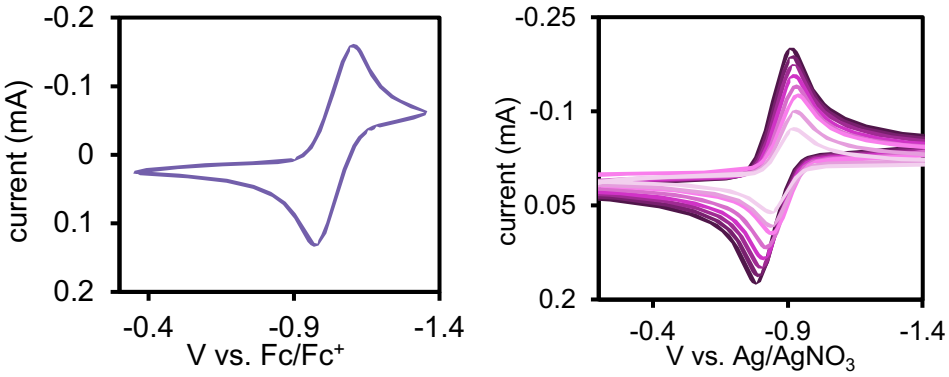

Figure S2. Cyclic voltammograms of 5 mM PQ in 0.5 M $TBAPF_6$, DMF at a scan rate of (left) 400 mV/s and (right) at 50, 100, 200, 300, 400, 500, 600, 700, and 800 mV/s referenced against $Ag/AgNO_3$.

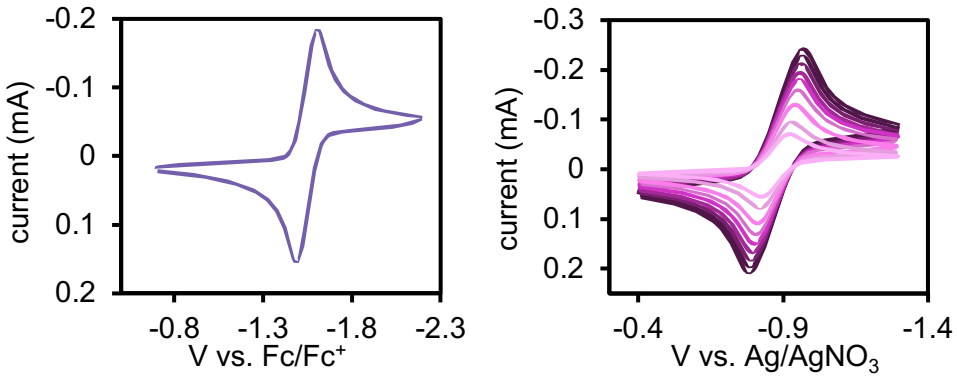

Figure S3. Cyclic voltammograms of 5 mM benzil in 0.5 M $TBAPF_6$, DMF at a scan rate of (left) 400 mV/s and (right) at 50, 100, 200, 300, 400, 500, 600, 700, and 800 mV/s referenced against $Ag/AgNO_3$.

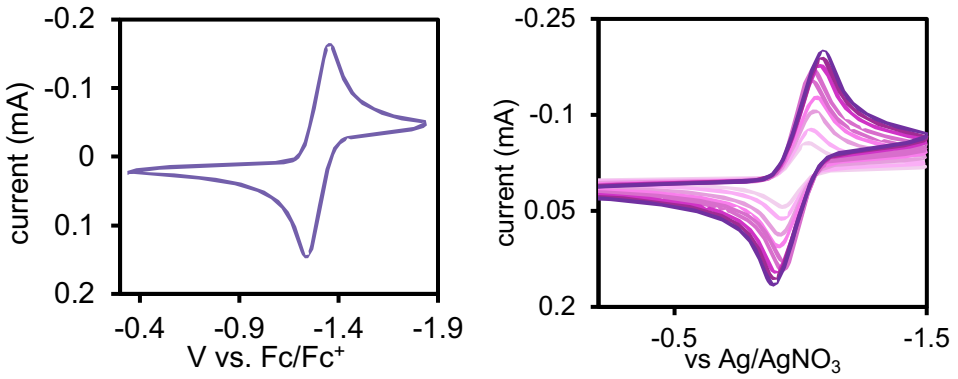

Figure S4. Cyclic voltammograms of 5 mM ANQ in 0.5 M $TBAPF_6$, DMF at a scan rate of (left) 400 mV/s and (right) at 50, 100, 200, 300, 400, 500, 600, 700, and 800 mV/s referenced against $Ag/AgNO_3$.

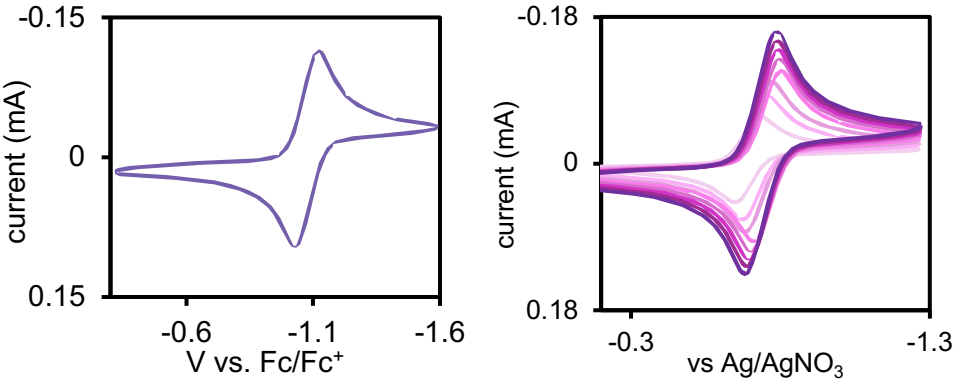

Figure S5. Cyclic voltammograms of 5 mM 2,2'-BDTP in 0.5 M $TBAPF_6$, DMF at a scan rate of (left) 400 mV/s and (right) at 50, 100, 200, 300, 400, 500, 600, 700, and 800 mV/s referenced against $Ag/AgNO_3$.

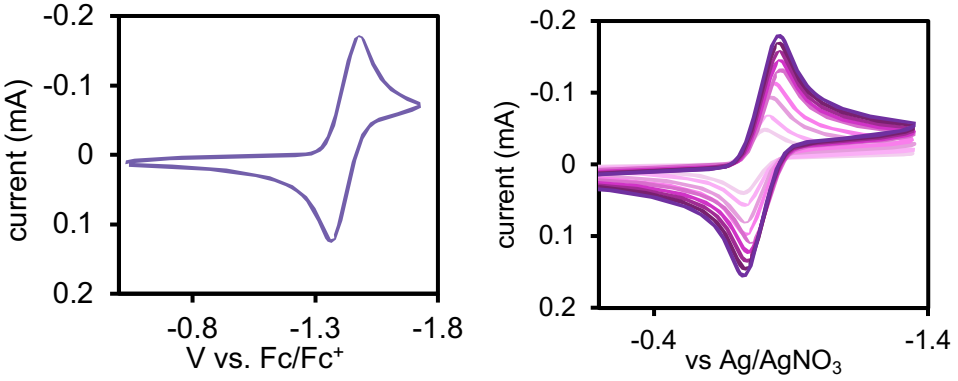

Figure S6. Cyclic voltammograms of 5 mM furil in 0.5 M $TBAPF_6$, DMF at a scan rate of (left) 400 mV/s and (right) at 50, 100, 200, 300, 400, 500, 600, 700, and 800 mV/s referenced against $Ag/AgNO_3$.

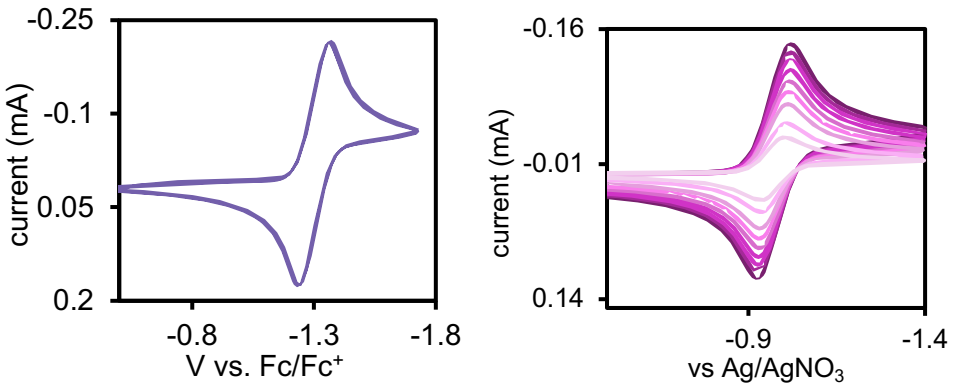

Figure S7. Cyclic voltammograms of 5 mM 2,2'-thenil in 0.5 M $TBAPF_6$, DMF at a scan rate of (left) 400 mV/s and (right) at 50, 100, 200, 300, 400, 500, 600, 700, and 800 mV/s referenced against $Ag/AgNO_3$.

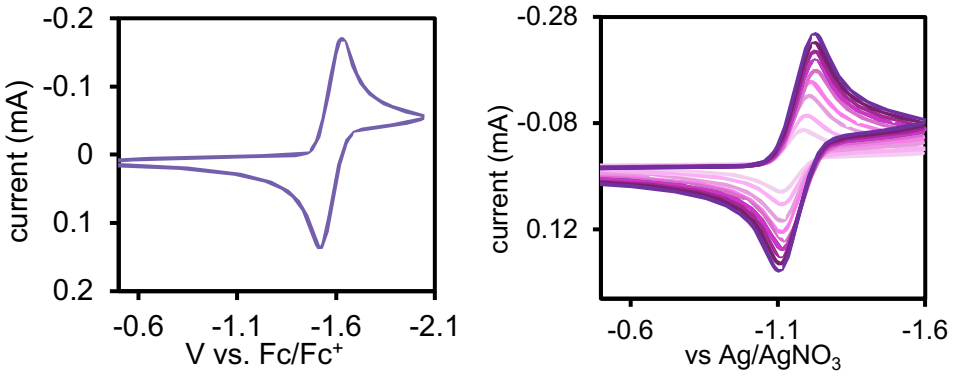

Figure S8. Cyclic voltammograms of 5 mM 3,3'-thenil in 0.5 M $TBAPF_6$, DMF at a scan rate of (left) 400 mV/s and (right) at 50, 100, 200, 300, 400, 500, 600, 700, and 800 mV/s referenced against $Ag/AgNO_3$.

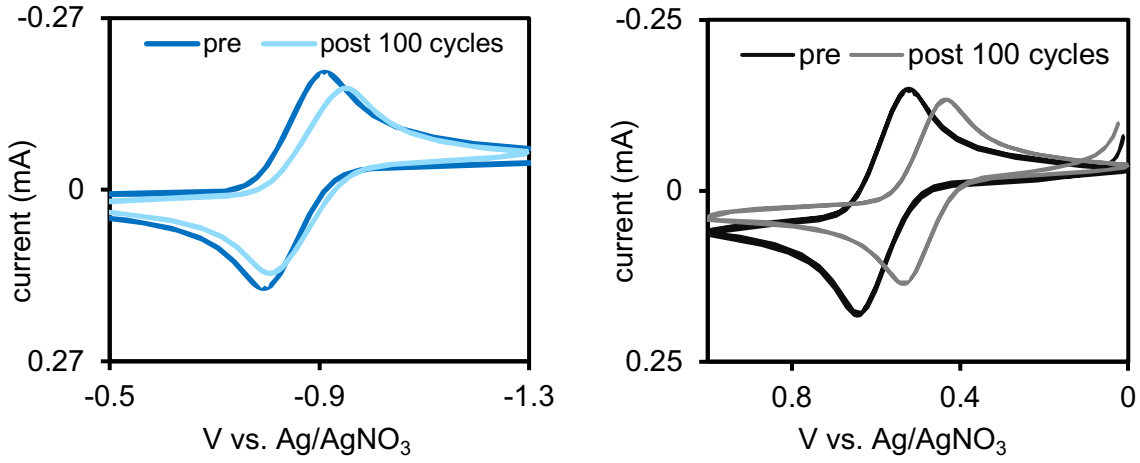

Figure S9. Cyclic Voltammograms of the working side pre and post 100 H-cells cycles containing 5 mM benzil (left) and of the counter side pre and post 100 H-cell cycles containing 5 mM ferrocene in 0.5 M $TBAPF_6$ referenced against $Ag/AgNO_3$.

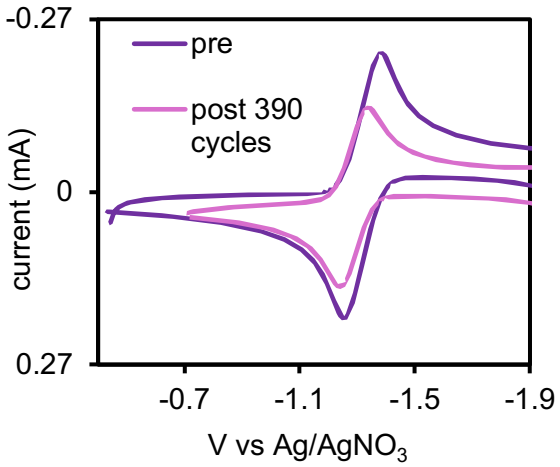

Figure S10. Cyclic Voltammograms of the working side pre and post 390 H-cells cycles containing 5 mM 2,2'-thenil (left) in 0.5 M $TBAPF_6$ referenced against $Ag/AgNO_3$.

Kinetic calculation plots

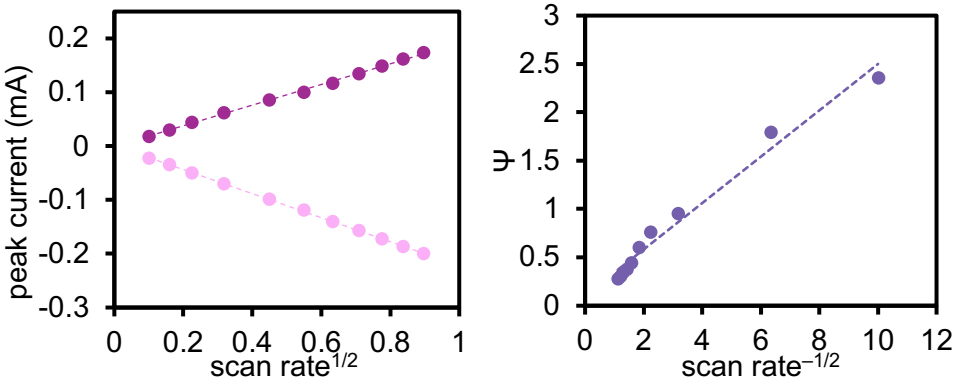

Figure S11. Plot of peak currents vs. $\nu^{1/2}$ used to determine the diffusion coefficients of PQ (left). Plot of the dimensionless parameter, Ψ vs. $\nu^{-1/2}$ used to determine the electron transfer rate constants k_0 with the Nicholson method of PQ (right).

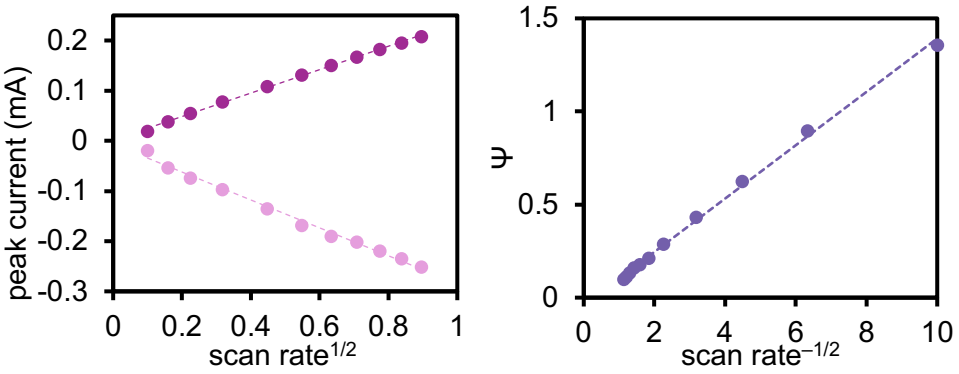

Figure S12. Plot of peak currents vs. $\nu^{1/2}$ used to determine the diffusion coefficients of benzil (left). Plot of the dimensionless parameter, Ψ vs. $\nu^{-1/2}$ used to determine the electron transfer rate constants k_0 with the Nicholson method of benzil (right).

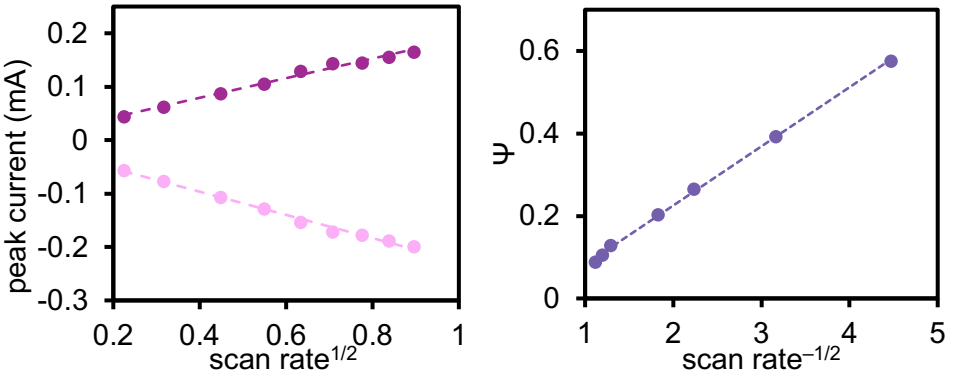

Figure S13. Plot of peak currents vs. $\nu^{1/2}$ used to determine the diffusion coefficients of ANQ (left). Plot of the dimensionless parameter, Ψ vs. $\nu^{-1/2}$ used to determine the electron transfer rate constants k_0 with the Nicholson method of ANQ (right).

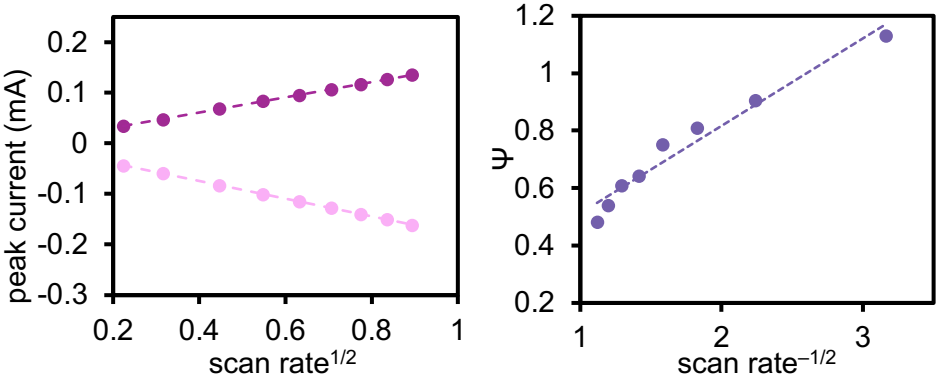

Figure S14. Plot of peak currents vs. $\nu^{1/2}$ used to determine the diffusion coefficients of 2,2'-BDTP (left). Plot of the dimensionless parameter, Ψ vs. $\nu^{-1/2}$ used to determine the electron transfer rate constants k_0 with the Nicholson method of 2,2'-BDTP (right).

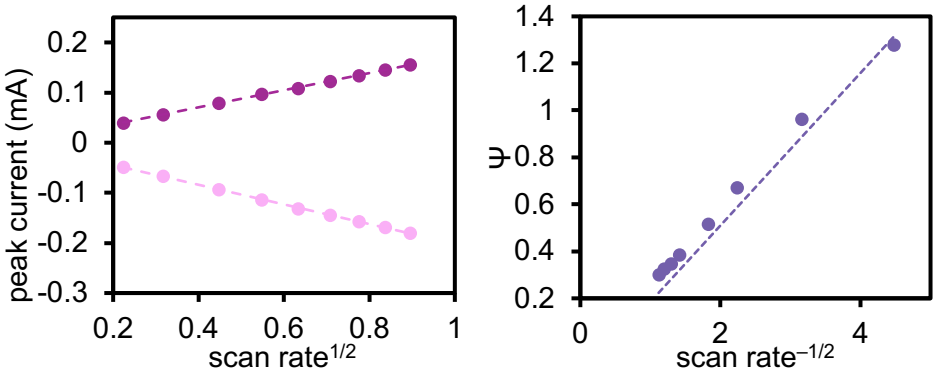

Figure S15. Plot of peak currents vs. $\nu^{1/2}$ used to determine the diffusion coefficients of furil (left). Plot of the dimensionless parameter, Ψ vs. $\nu^{-1/2}$ used to determine the electron transfer rate constants k_0 with the Nicholson method of furil (right).

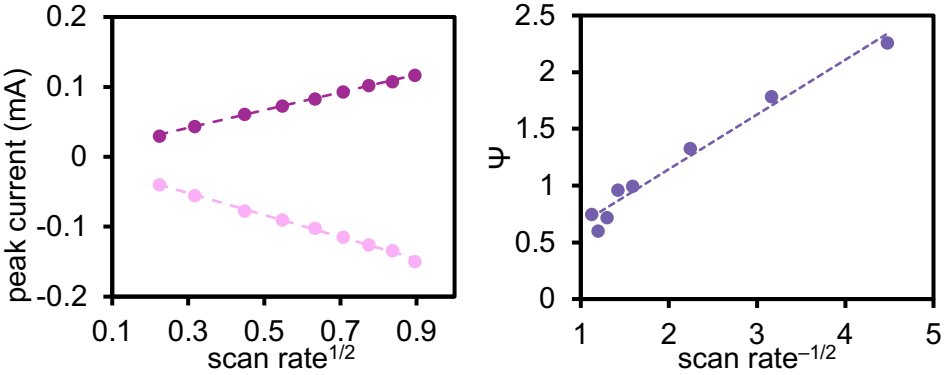

Figure S16. Plot of peak currents vs. $\nu^{1/2}$ used to determine the diffusion coefficients of 2,2'-thenil (left). Plot of the dimensionless parameter, Ψ vs. $\nu^{-1/2}$ used to determine the electron transfer rate constants k_0 with the Nicholson method of 2,2'-thenil (right).

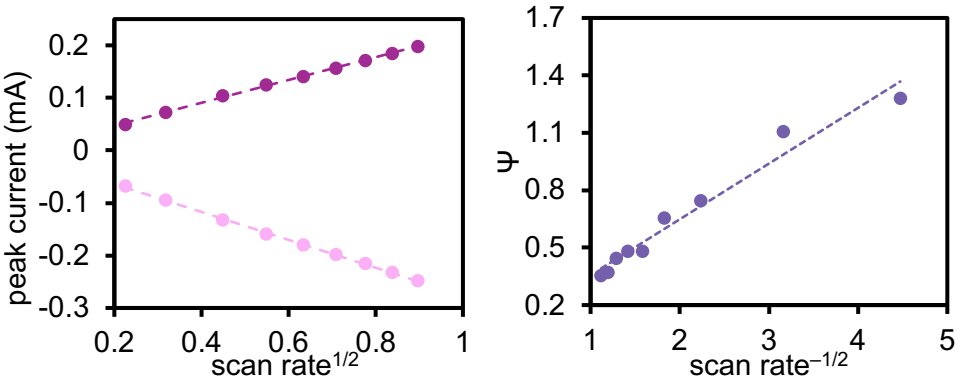

Figure S17. Plot of peak currents vs. $\nu^{1/2}$ used to determine the diffusion coefficients of 3,3'-thenil (left). Plot of the dimensionless parameter, Ψ vs. $\nu^{-1/2}$ used to determine the electron transfer rate constants k_0 with the Nicholson method of 3,3'-thenil (right).

Charge/discharge Cycling Experimental Methods

H-cell cycling. Charge/discharge experiments were performed in a N_2 filled glovebox on a Biologic VSP multichannel potentiostat/galvanostat. Cycling was performed in a custom glass H-cell with a porous glass frit separator (P5, Adams and Chittenden), reticulated vitreous carbon working and counter electrodes (100 ppi, Duocell, total 2.8 x 0.6 cm, ~ 2 x 0.6 cm under the solution surface, 0.6 cm thick) and an Ag/Ag^+ quasi-reference electrode (BASi) filled with the solvent/electrolyte solution being used. Each chamber was loaded with 5 mL of solution, with a supporting electrolyte concentration of 500 mM and 5 mM of ROM. The working electrode chamber contained the reference electrode and tested anolytes, while the counter chamber contained one equivalence of ferrocene, both chambers were stirred during the full length of the experiment. The constant current constant voltage (CCCV) program was used, a current of |3mA| was applied *via* the RVC electrodes. Cycling boundaries of 70% SoC or the set voltage, +/– 0.2 – 0.3 V, from $E_{1/2}$ were employed in the CC step. If the CV step was triggered, this continued until 70% SoC was hit or a near zero current was obtained.

CCCV is considered the standard charging/discharging method for lithium-ion batteries and has been utilized in other battery reports.[4–6] The CCCV method was utilized instead of a constant current (CC) method without the potential hold to assess cycling stabilities with greater material utilization. With the CC method charging and discharging at |0.3mA|, the maximum state of charge reached for benzil was 60% (Figure S38). The static H-cell used contains a porous glass frit to separate the compartments instead of a membrane, and the solution is stirred with a stir bar instead of constant flow. This set-up, although minimizing cross-over, leads to greater resistance than in a flow cell. Cycling studies with a flow cell was attempted. However, the lack of materials for our flow cell with long-term chemical resistance against non-aqueous conditions, hindered flow cell cycling studies. The CCCV method enabled accessing greater state of charges, which provided a better comparison of cycling stability across the tested anolytes when a feasible flow cell set-up was not available. We acknowledge that static H-cell studies are not representative of cycling under flow conditions, especially for capacity fade through cross-over and higher concentrations. We have been and will continue to engineer a non-aqueous flow cell system to test these anolytes in a flow cell.

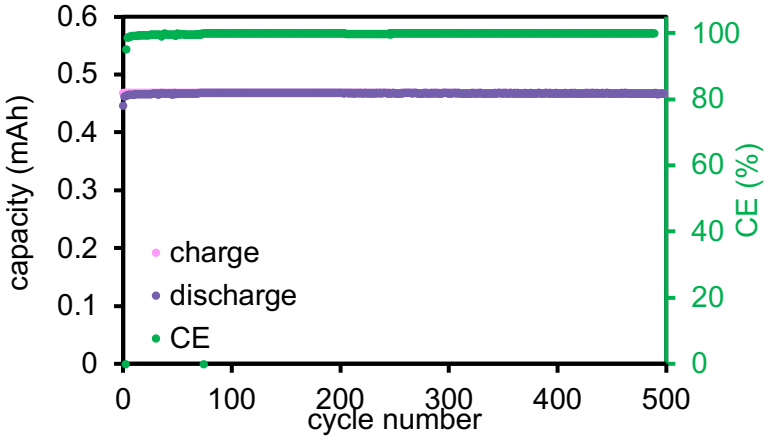

Figure S18. H-cell charging and discharging cycles of 5 ml of 5 mM benzil in 0.5 M $TBAPF_6$, DMF (theoretical capacity of 0.67 mAh) and coulombic efficiencies.

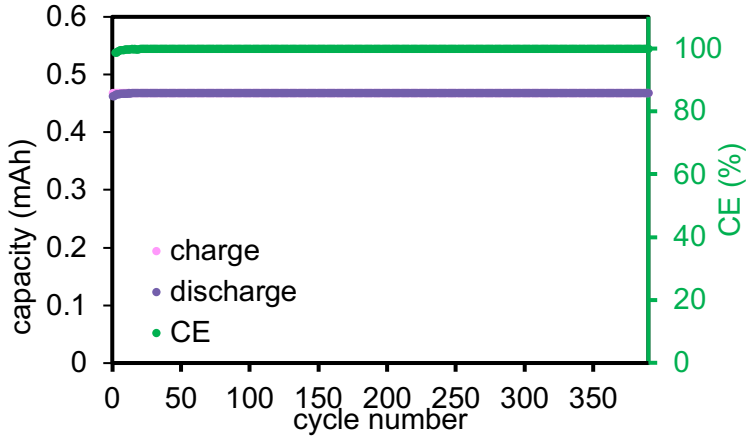

Figure S19. H-cell charging and discharging cycles of 5 ml of 5 mM 2,2'-thenil in 0.5 M $TBAPF_6$, DMF (theoretical capacity of 0.67 mAh) and coulombic efficiencies.

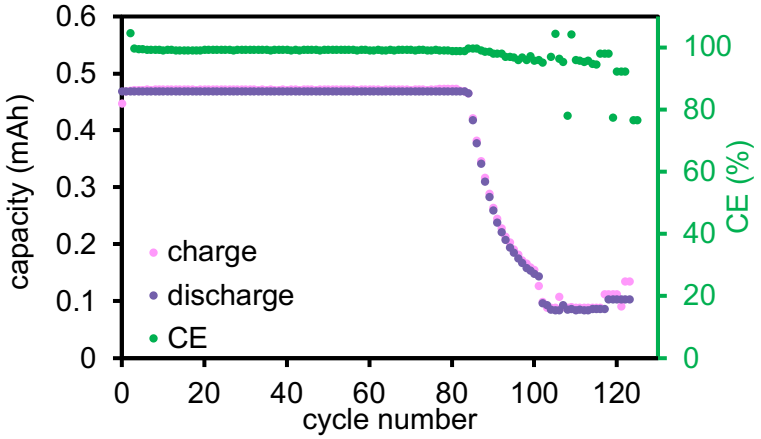

Figure S20. H-cell charging and discharging cycles of 5 ml of 5 mM PQ in 0.5 M $TBAPF_6$, DMF (theoretical capacity of 0.67 mAh) and coulombic efficiencies.

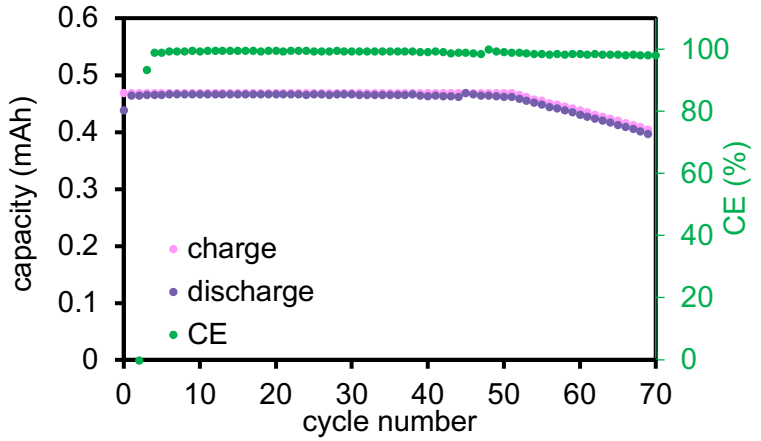

Figure S21. H-cell charging and discharging cycles of 5 ml of 5 mM ANQ in 0.5 M $TBAPF_6$, DMF (theoretical capacity of 0.67 mAh) and coulombic efficiencies.

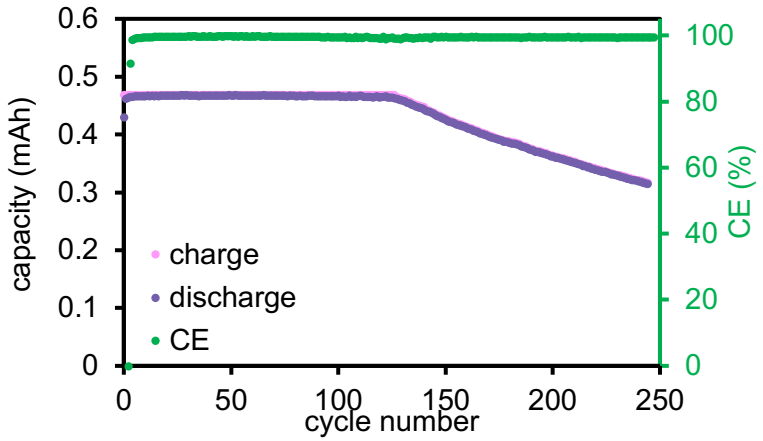

Figure S22. H-cell charging and discharging cycles of 5 ml of 5 mM furil in 0.5 M $TBAPF_6$, DMF (theoretical capacity of 0.67 mAh) and coulombic efficiencies.

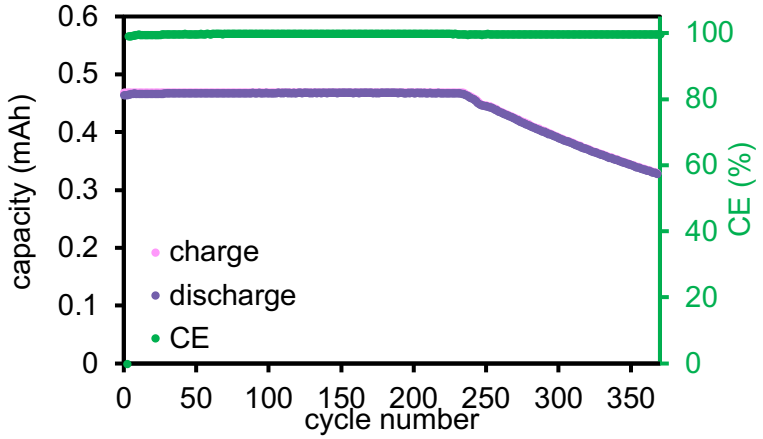

Figure S23. H-cell charging and discharging cycles of 5 ml of 5 mM 3,3'-thenil in 0.5 M $TBAPF_6$, DMF (theoretical capacity of 0.67 mAh) and coulombic efficiencies.

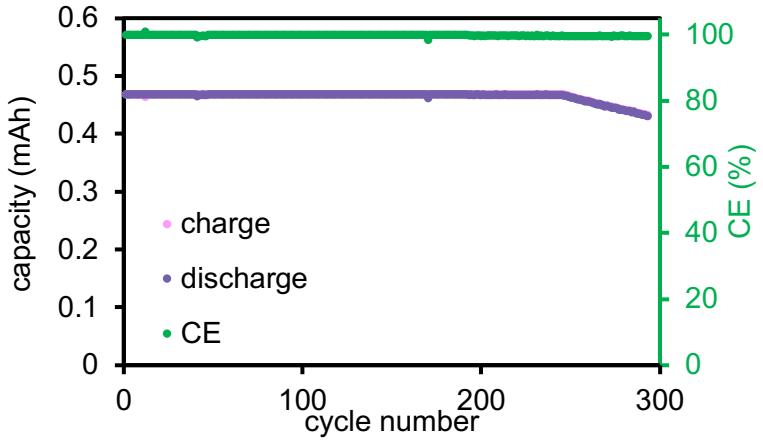

Figure S24. H-cell charging and discharging cycles of 5 ml of 5 mM 2,2'-BDTP in 0.5 M $TBAPF_6$, DMF (theoretical capacity of 0.67 mAh) and coulombic efficiencies.

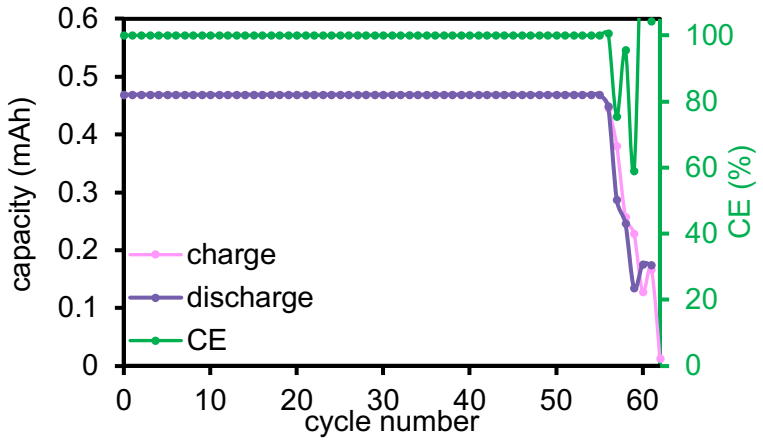

Figure S25. H-cell charging and discharging cycles of 5 ml of 5 mM 4,4'-BDTP in 0.5 M $TBAPF_6$, DMF (theoretical capacity of 0.67 mAh) and coulombic efficiencies.

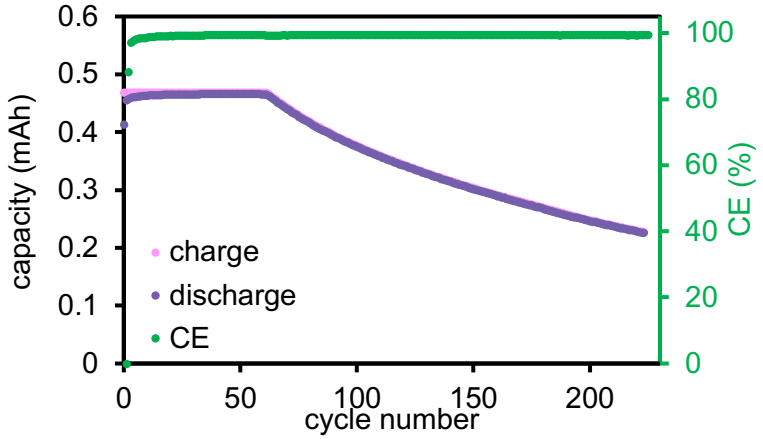

Figure S26. H-cell charging and discharging cycles of 5 ml of 5 mM benzil in 0.5 M LiTFSI, DMF (theoretical capacity of 0.67 mAh) and coulombic efficiencies.

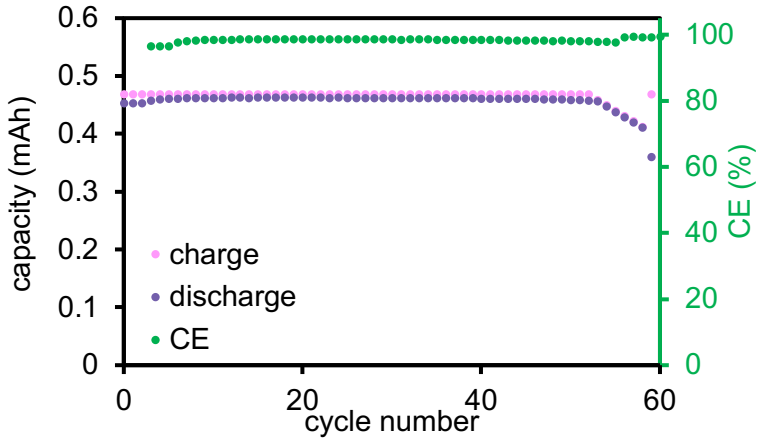

Figure S27. H-cell charging and discharging cycles of 5 ml of 5 mM benzil in 0.5 M KPF_6, DMF (theoretical capacity of 0.67 mAh) and coulombic efficiencies.

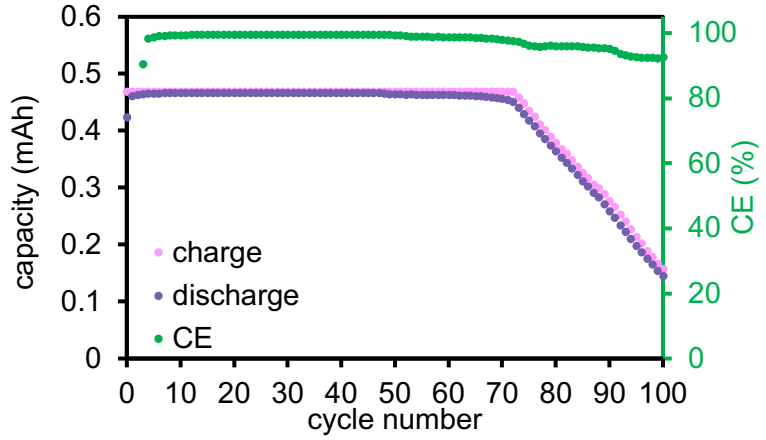

Figure S28. H-cell charging and discharging cycles of 5 ml of 5 mM benzil in 0.25 M $TBABF_4$, DMF (theoretical capacity of 0.67 mAh) and coulombic efficiencies.

H-cell cycling voltage profiles

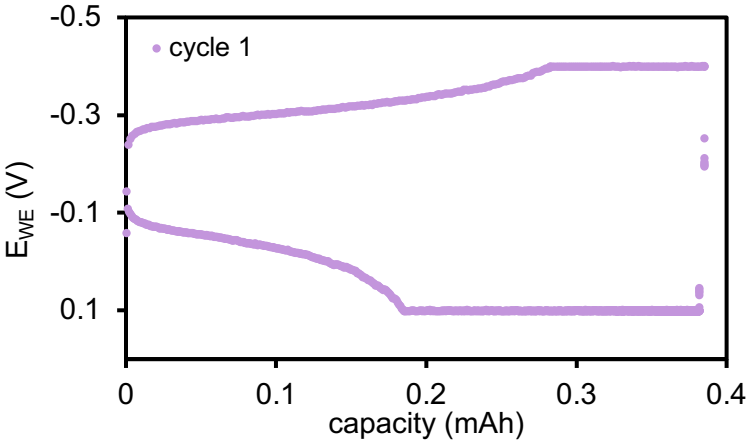

Figure S29. Voltage profile of PQ H-cell cycling in 0.5 M $TBAPF_6$, DMF on cycle 1. Constant current constant voltage (CCCV) is employed to allow for full charge and discharges without large amounts of overpotential being added to the system.

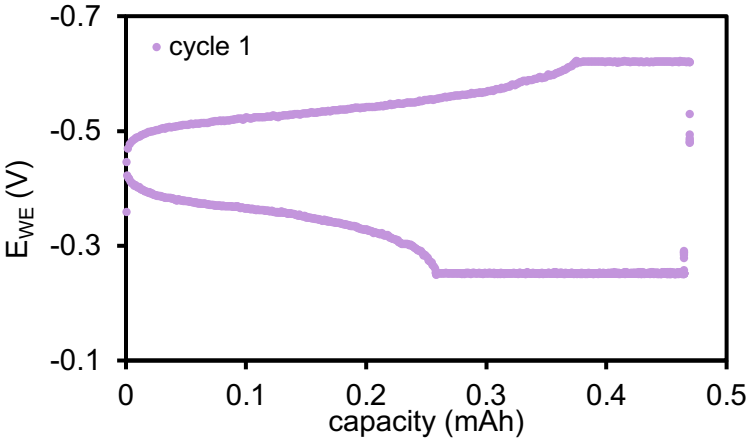

Figure S30. Voltage profile of ANQ H-cell cycling in 0.5 M $TBAPF_6$, DMF on cycle 1.

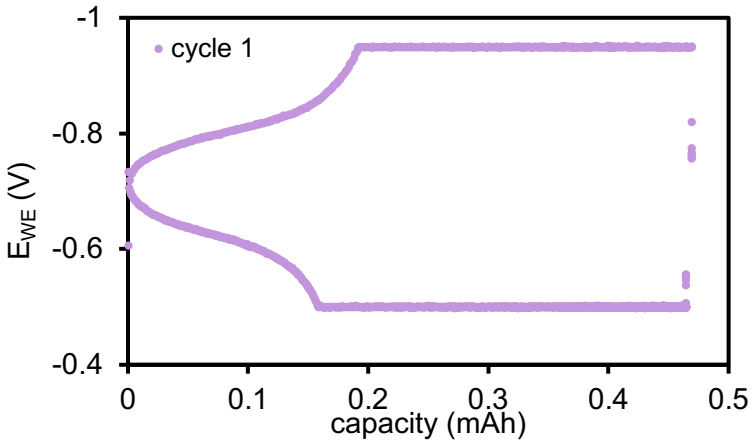

Figure S31. Voltage profile of furil H-cell cycling in 0.5 M $TBAPF_6$, DMF on cycle 1.

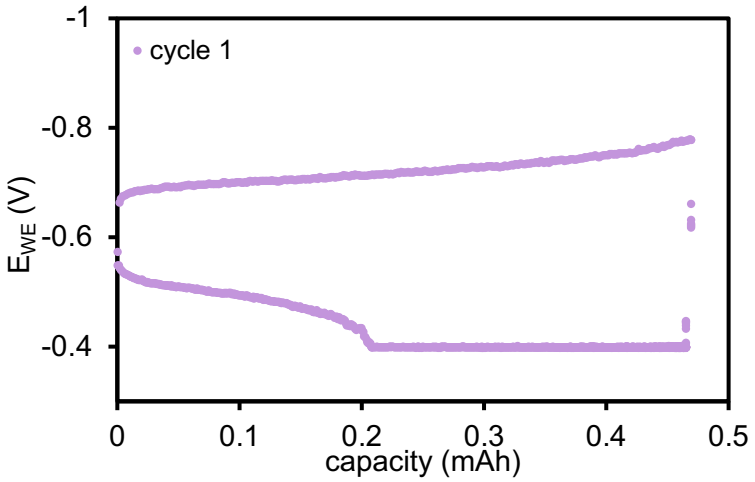

Figure S32. Voltage profile of 2,2'-thenil H-cell cycling in 0.5 M $TBAPF_6$, DMF on cycle 1.

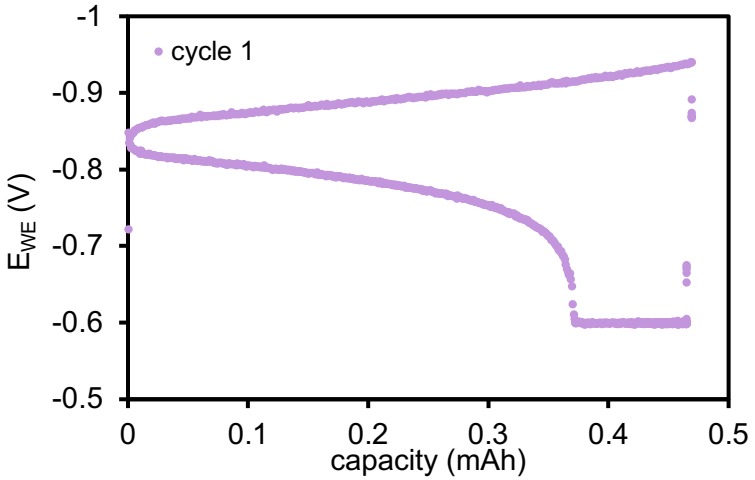

Figure S33. Voltage profile of 3,3'-thenil H-cell cycling in 0.5 M $TBAPF_6$, DMF on cycle 1.

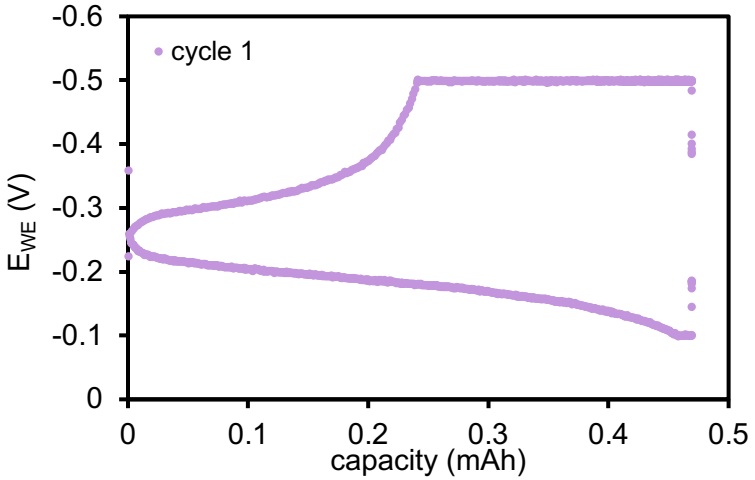

Figure S34. Voltage profile of 2,2'-BDTP H-cell cycling in 0.5 M $TBAPF_6$, DMF on cycle 1.

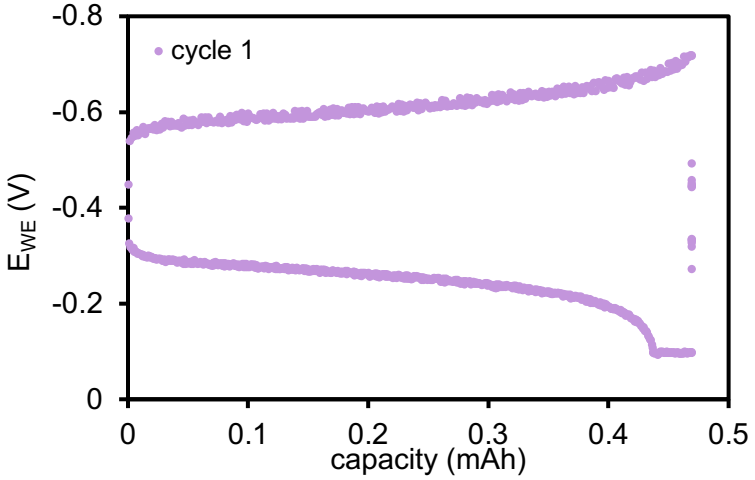

Figure S35. Voltage profile of 4,4'-BDTP H-cell cycling in 0.5 M $TBAPF_6$, DMF on cycle 1.

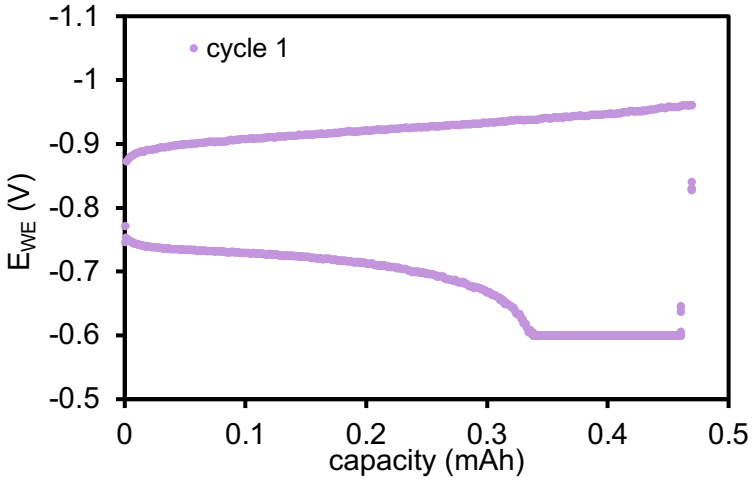

Figure S36. Voltage profile of benzil H-cell cycling in 0.5 M LiTFSI, DMF on cycle 1.

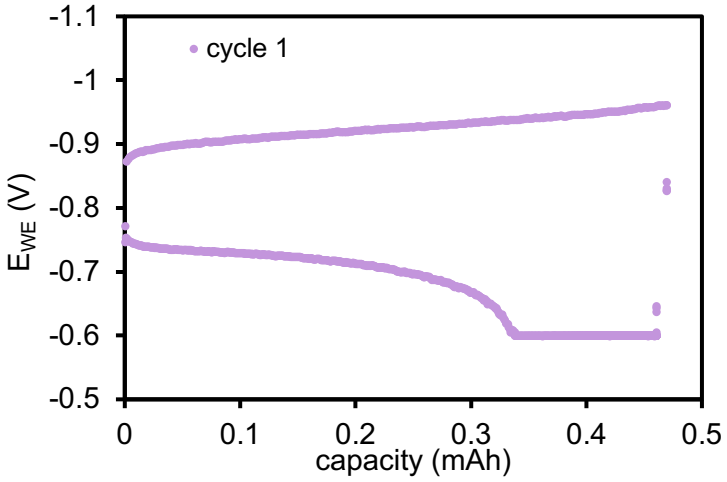

Figure S37. Voltage profile of benzil H-cell cycling in 0.5 M KPF_6, DMF on cycle 1.

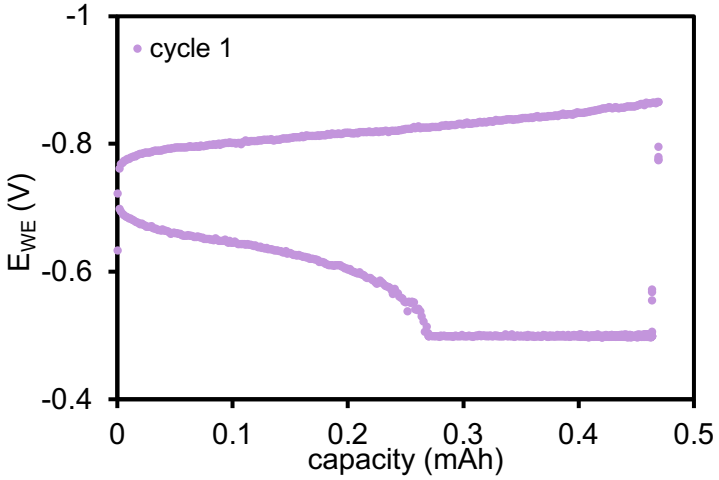

Figure S38. Voltage profile of benzil H-cell cycling in 0.25 M $TBABF_4$, DMF on cycle 1.

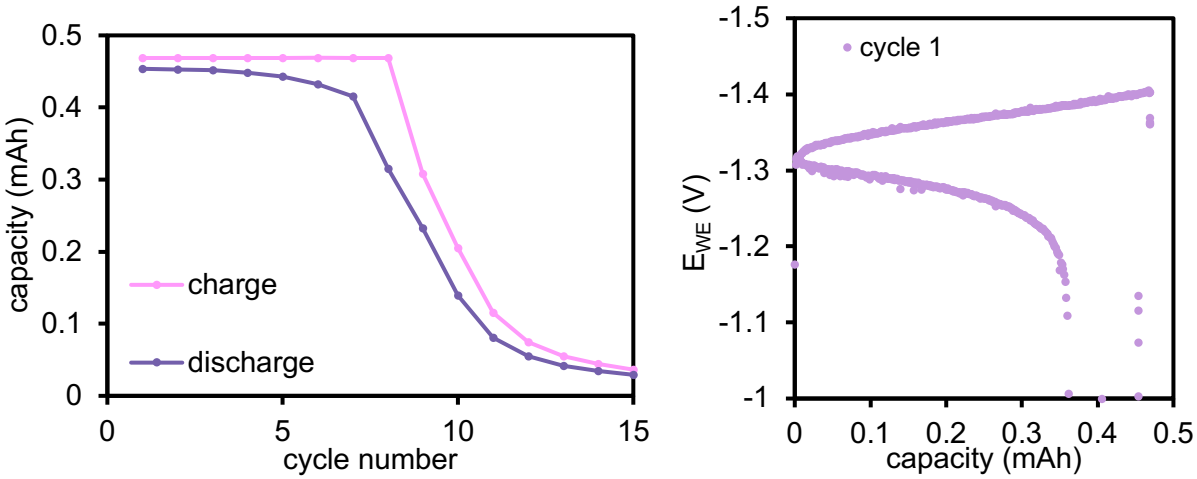

Figure S39. H-cell charging and discharging cycles of 5 ml of 5 mM benzil in 0.5 M $TBAPF_6$, MeCN (theoretical capacity of 0.67 mAh) (left) and voltage profile at cycle 1 (right).

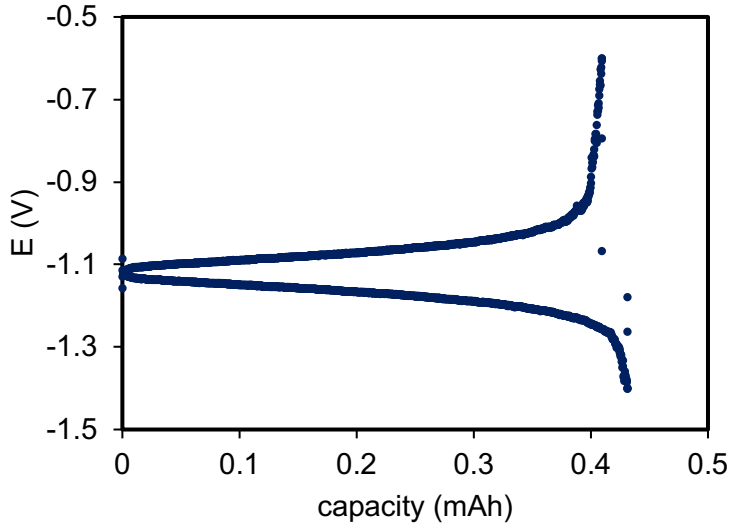

Figure S40. Voltage profile of a CC cycling method of 5 ml of 5 mM benzil in 0.5 M $TBAPF_6$, DMF (theoretical capacity of 0.67 mAh).

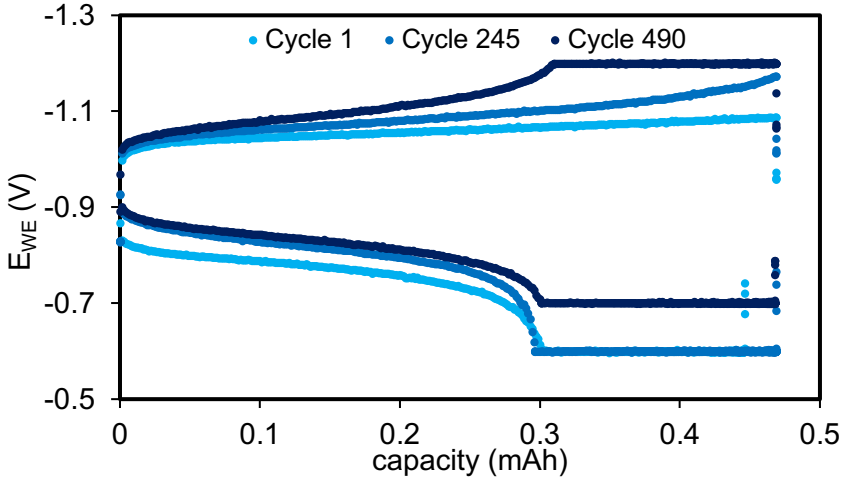

Figure S41. Voltage profile of a CCCV H-cell cycling of 5 mM benzil in 0.5 M $TBAPF_6$, DMF on cycle 1, 245, and 490.

EPR Measurements and Simulations

EPR of benzil radical anion. EPR measurements of the radical anion was prepared by the following procedure. 2.5 mM benzil was electrochemically reduced in 0.5 M $TBAPF_6$ and DMF in an H-cell in a N_2 filled glovebox. This solution was diluted with DMF to 0.625 mM benzil 0.125 M $TBAPF_6$ and transferred to a round quartz capillary tube (0.60 ID x 0.84 OD, VitroTubes™). CW EPR measurements were carried out at room temperature with a Bruker EMX X-band spectrometer operating at 9.8 GHz (EMX; Bruker Biospin, Billerica, MA) and a dielectric cavity (ER 4123D; Bruker Biospin, Billerica,

MA). A sample of 10.0 µL volume was loaded into a quartz capillary tube with 0.6 mm internal diameter (CV6084; VitroCom), sealed at one end with critoseal, and then placed in the dielectric cavity for measurements. CW EPR spectra were acquired by using 2 mW of microwave power, 0.5 gauss modulation amplitude, 200 gauss sweep width, and 10 scans of signal averaging. EPR simulations were conducted on EasySpin.[7,8]

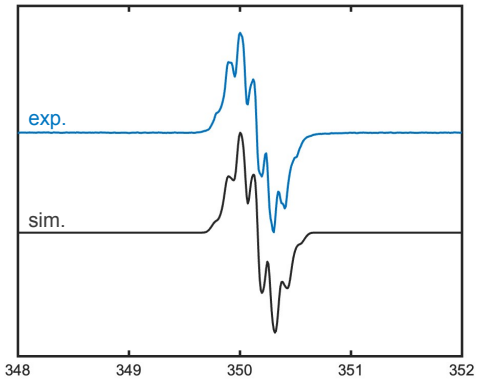

Figure S42. EPR spectrum of 0.625 mM benzil radical anion in 0.125 M $TBAPF_6$, DMF. Simulation parameters: S = 1/2, g = 1.9945, 4 x $A(^1H)$ = 3.0 MHz, 4 x $A(^1H)$ = 1.1 MHz, 2 x $A(^1H)$ = 3.18 MHz.

IR Measurements

Infrared spectroscopy of neutral benzil and radical anion: Fourier-transform infrared spectroscopy (FT-IR) of the neutral and reduced benzil species was performed with a Thermo Scientific Nicolet iS50 infrared spectrometer using a liquid-nitrogen cooled MCT/A detector with CaF_2 window and KBr beamsplitter. Transmission mode was used with an International Crystal Laboratories liquid FT-IR cell using CaF_2 windows and a 200 µm Teflon spacer. Background spectra were collected using aliquots of identical solution used for sample prior to benzil addition. Background spectra were nominally 100 mM $TBAPF_6$ in deuterated DMSO (Cambridge Isotopes). Sample spectra were collected at a concentration of 20 mM benzil.

The radical anion was generated electrochemically. A three-electrode H-cell with porous glass frit divider was used in a N_2 filled glovebox (H_2O and O_2 both <0.1 ppm), with 20 mM benzil in d-DMSO in the cathode chamber and 20 mM ferrocene in d-DMSO in the anode chamber. The reference electrode was a Ag/Ag^+ quasireference. A constant current of 2 mA was flowed until a potential of 1.4 V vs Ag/Ag^+ was obtained (corresponding to the first reduction) at which point the potential was held constant to prevent over-reduction to the dianion until 1.9 mAh of charge was passed, corresponding to approximately 73% of theoretical capacity (maximum theoretical capacity = 2.6 mAh). The catholyte changes from a light yellow-green (neutral benzil) to dark blue (radical anion) while the anolyte begins as bright orange (ferrocene) and becomes dark green (ferrocenium). The transmission IR cell was assembled inside the glovebox and sample was injected into the chamber also inside the glovebox. The IR cell was sealed with Teflon plugs

and transferred to a sealed plastic bag to prevent O_2 contamination before being removed from the glovebox and transported to the FT-IR where spectra were immediately collected.

The electrochemically generated benzil radical anion solution was prepared as stated in the measurement of the IR spectrum above. 1 ml of the sample solution was sealed in a CaF_2 window cell inside an N_2 glovebox. The Raman measurement conditions were, 266 nm at 7 mW, UV-enhanced 2400 line/mm grating, 15 msec exposure (90 msec for neutral benzil sample).

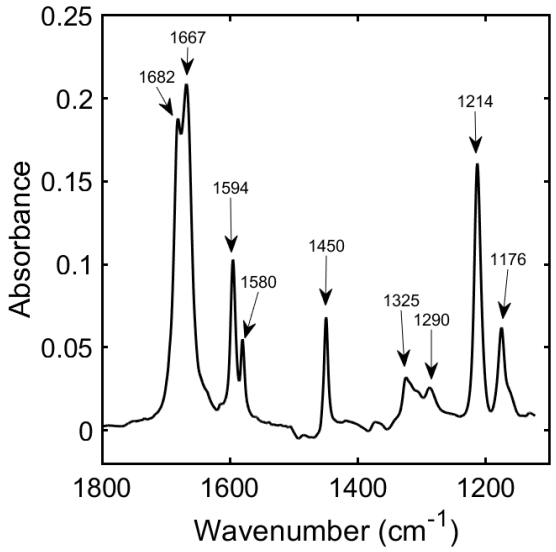

Figure S43. IR spectrum of 20 mM benzil in d-DMSO with peak positions annotated.

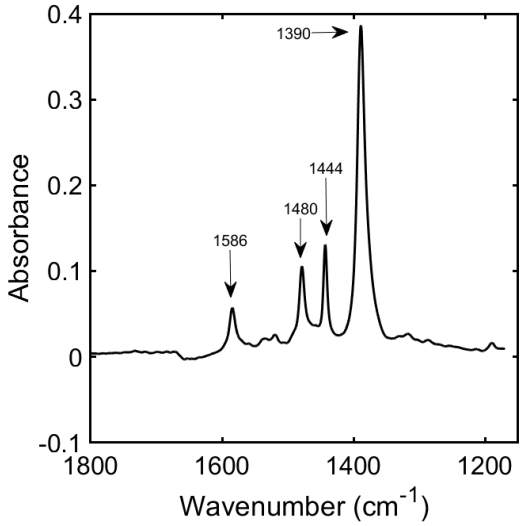

Figure S44. IR spectrum of 20 mM electrochemically generated benzil radical anion with peak positions annotated.

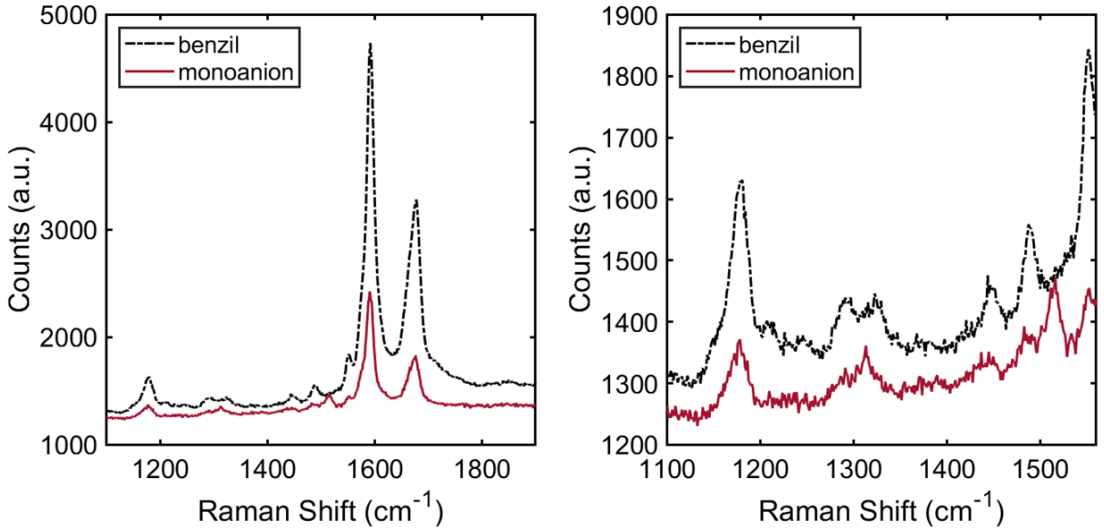

Figure S45. Raman infrared spectra of 20 mM benzil, 100 mM $TBAPF_6$ in DMSO-d_6. Black trace is neutral molecule, red trace is benzil reduced electrochemically via potential-limited electrolysis.

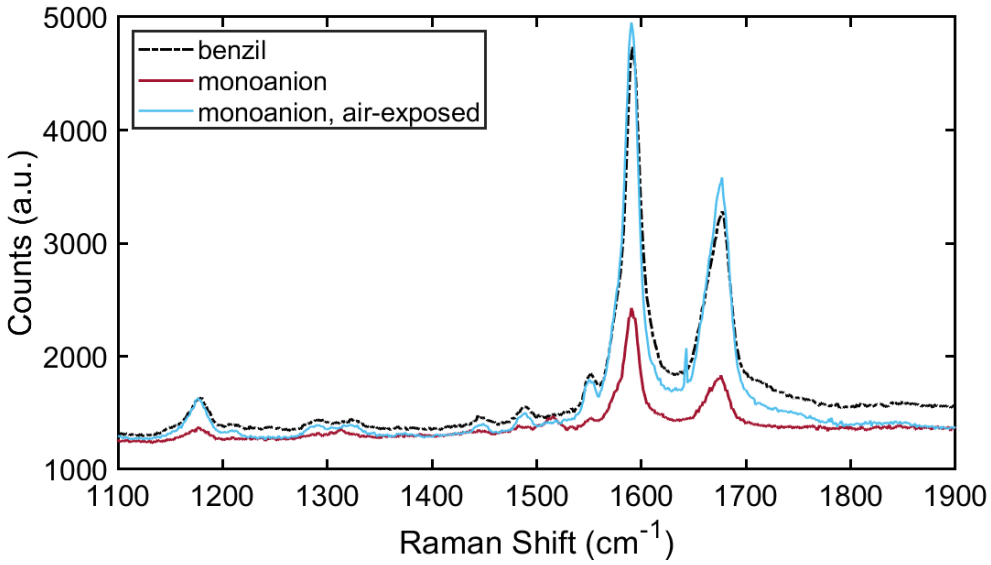

Figure S46. Raman infrared spectra of 20 mM benzil, 100 mM $TBAPF_6$ in DMSO-d_6. Black trace is neutral molecule, red trace is benzil reduced electrochemically via potential-limited electrolysis, blue trace is monoanion sample after brief (~10 s) exposure to air.

Table S3. FT-IR data for neutral benzil with vibration assignments

Wavenumber (cm^{-1})	Assignment
1682/1667	ν(C=O) antisymmetric/symmetric
1594/1580	8a/b (C-C stretch, ring)
1450	19b (C-H bend, ring)
1325	3 (C-C stretch, ring)

1290	ν(C-Ph), antisymmetric
1214	ν(C-Ph), symmetric
1176	9a (C-H bend, ring)

Assignments based on literature precedent.[9–12] *Spectroscopic notation is v = stretching mode, others are Wilson's notation with approximate descriptions written out.*[13]

Table S4. FT-IR data for benzil radical anion with vibration assignments

Wavenumber (cm^{-1})	Assignment
1586	8a/b (C-C stretch, ring)
1480	19a (C-H bend, ring)
1444	19b (C-H bend, ring)
1390	ν(C=O) antisymmetric

Assignments based on literature precedent.[9,10,12] *Spectroscopic notation is v = stretching mode, others are Wilson's notation with approximate descriptions written out.*[13]

Table S5. Raman data for neutral benzil with vibration assignments

Raman shift(cm^{-1})	Assignment
1673	ν(C=O) antisymmetric
1591	ν(C=O) symmetric
1550	8a (C-C, ring)
1487	19a (C-H bend, ring)
1443	19b (C-H bend, ring)
1322	3 (C-H bend, ring)
1290	ν C-Ph), symmetric
1176	9a (C-H bend, ring)

Assignments based on literature precedent.[9,10,12,14–16] *Spectroscopic notation is v = stretching mode, others are Wilson's notation with approximate descriptions written out*[13]

Table S6. Raman data for benzil radical anion with vibration assignments

Raman Shift (cm^{-1})	Assignment
1673	ν(C=O) antisymmetric (cis-skewed)
1591	ν(C=O) symmetric (cis-skewed)
1517	ν(C=O) symmetric (trans-planar)
1312	ν (C-C)
1178	9a (C-H bend, ring)

Assignments based on literature precedent.[9,10,12,14,15] *Spectroscopic notation is v = stretching mode, others are Wilson's notation with approximate descriptions written out*[13]

Table S7. Character Table Analysis of benzil IR and Raman active bands

C_2 – *cis*-skewed benzil, reducible representation for C=O stretch

C_2	E	C_2
Γ_{CO}	2	0

Irreducible representation

C_2	E	C_2	functions	IR/Raman active?
Γ_{CO}	2	0		
A	+1	+1	z, x^2, y^2, z^2, xy	IR + Raman
B	+1	-1	x, y, yz, xz	IR + Raman

C_{2h} – *trans*-planar benzil, reducible representation for C=O stretch

C_{2h}	E	$C_2(z)$	i	σ_h
Γ_{CO}	2	0	0	2

Irreducible representation

C_{2h}	E	$C_2(z)$	i	σ_h	func	IR/Raman?
Γ_{CO}	2	0	0	2		
A_g	1	1	1	1	x^2, y^2, z^2, xy	Raman
B_u	1	-1	-1	1	x, y	IR

Computational Calculations

To account for non-covalent interactions, geometry optimization of ion-pair radical anions was performed with the ORCA computational chemistry package utilizing the B3LYP functional, D3 dispersion correction and def2-SVP basis set with CPCM solvation in DMF on the Northwestern University Quest high performance computing facility.[17–19] Avogadro: an open-source molecular builder and visualization tool. Version 1.2.0. http://avogadro.cc/ was used for visualizing optimized geometries and electron and spin densities.[20] The energy surface scanning dihedral angles and orbital calculations were conducted with *Rowan Scientific*. https://www.rowansci.com using the ωB97X-3c method, which utilizes the ωB97X-V functional with a def2-mTZVPP basis set.[21,22]

Table S8. Optimized dihedral angles of the neutral and radical anions with TBA^+

compound	Neutral dihedral angle (θ°)	Radical anion dihedral angle (θ°)
Benzil + TBA^+	91.2	179.9
Benzil + Li^+	109.2	10.8
Benzil + K^+		12.7
2,2'-thenil + TBA^+	137.7	182.3
3,3'-thenill + TBA^+	87.6	160.2
Furil + TBA^+	140.5	170.1

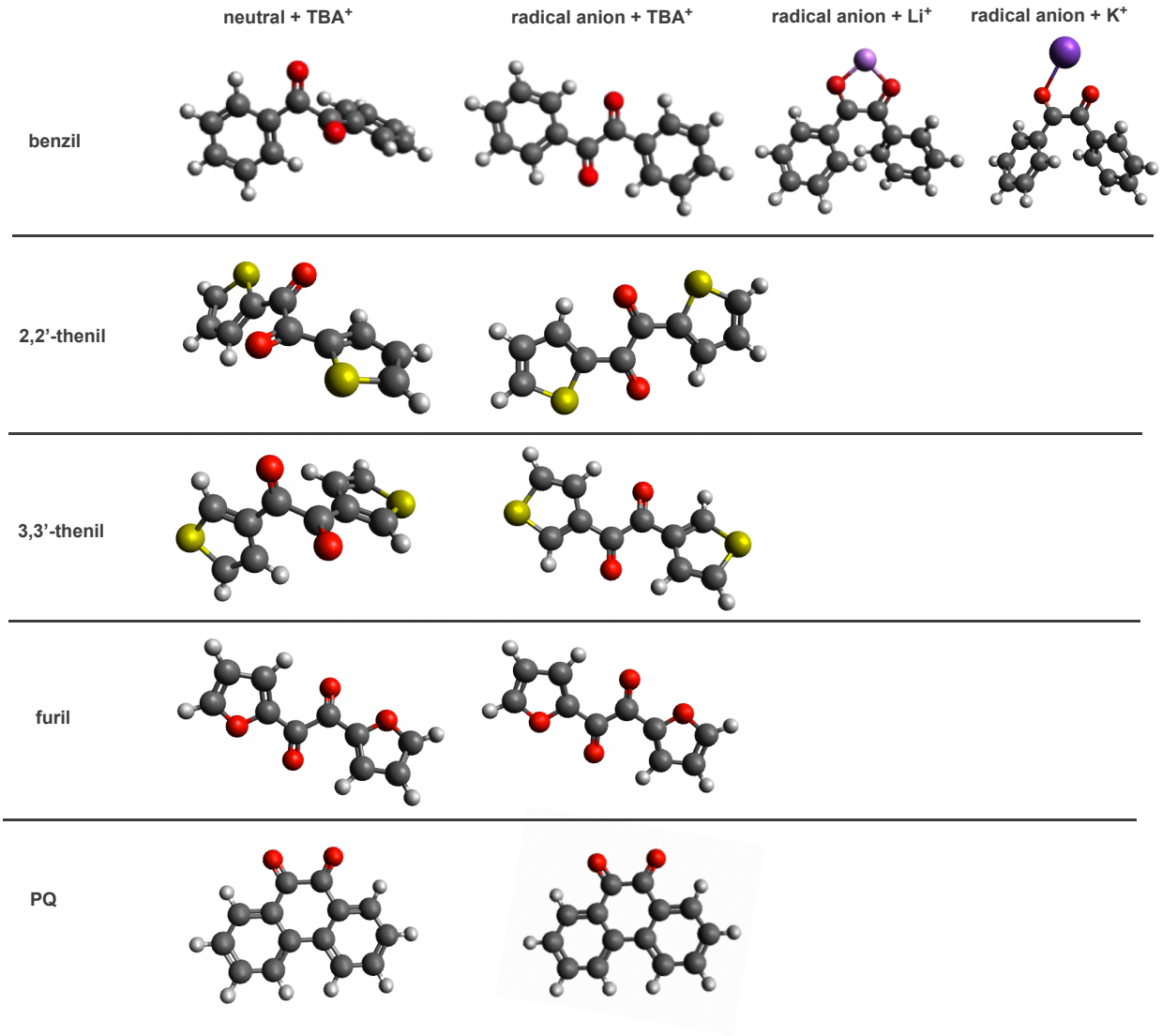

Figure S47. Optimized geometries of acylic 1,2-dicarbonyl and PQ neutral structures with TBA^+ and radical anions with TBA^+ or Li^+.

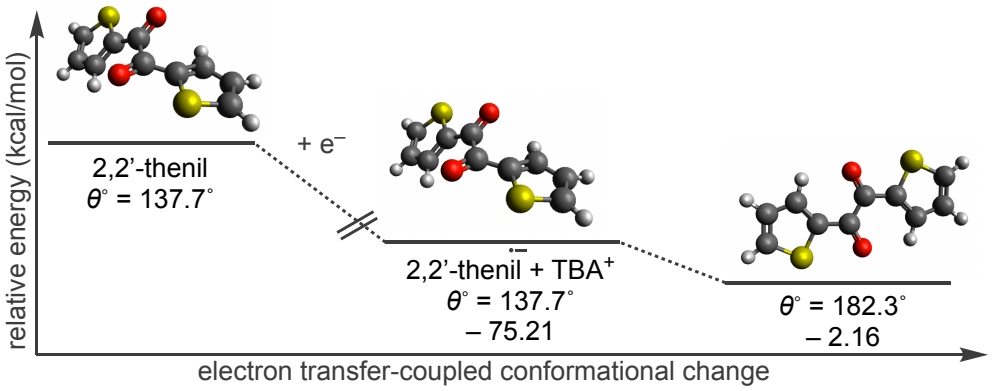

Figure S48. Reaction coordinates for the electron transfer-coupled conformational change of 2,2'-thenil

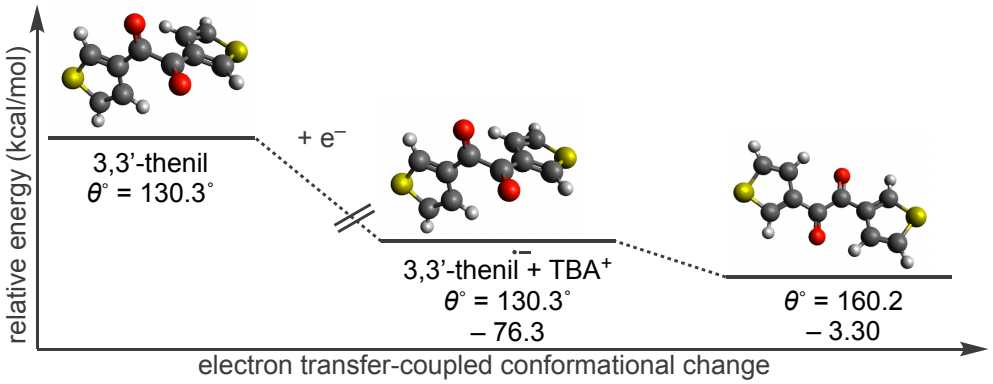

Figure S49. Reaction coordinates for the electron transfer-coupled conformational change of 3,3'-thenil

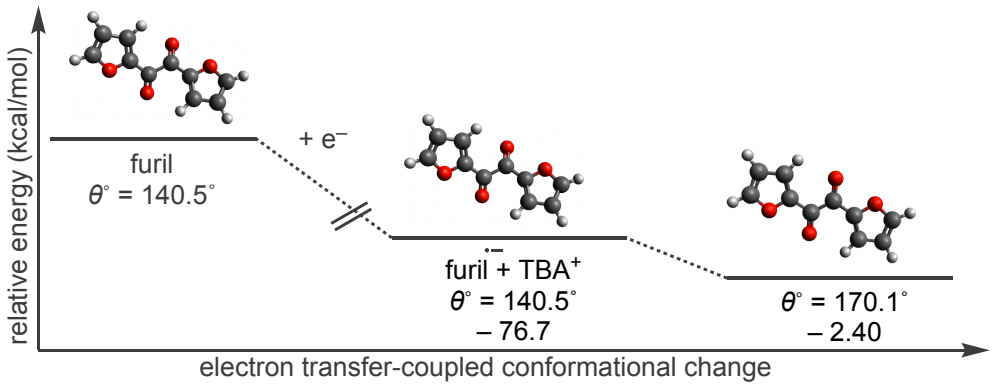

Figure S50. Reaction coordinates for the electron transfer-coupled conformational change of furil

Cartesian coordinates

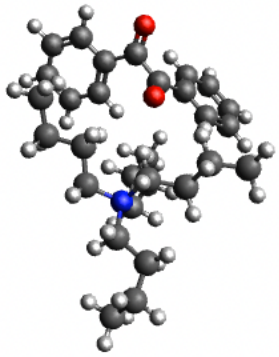

Figure S51. Optimized geometery of neutral benzil with TBA^+

Benzil neutral with TBA^+

O	1.1342907040	0.2294622460	0.5063721225
O	0.1521558627	2.2686751258	-1.5717135963
C	1.4580400562	-0.6711979170	-1.6833090339

C	-1.6783420998	0.8346240908	-1.0377790366
C	0.8167428336	0.1955445165	-0.6702575530
C	-0.2512785572	1.1950396959	-1.1486296027
C	0.9358928374	-0.7605757564	-2.9846448373
C	-2.0747471520	-0.4453556440	-0.6112369165
C	2.6022367571	-1.4116806094	-1.3367241086
C	-2.6501457218	1.7729629372	-1.4297347248
C	1.5561159537	-1.5705737639	-3.9357711166
C	-3.4292261489	-0.7823275850	-0.5870139486
C	3.2230223820	-2.2169281521	-2.2891946018
C	-3.9997252513	1.4345481666	-1.4052108242
C	2.7024766861	-2.2944085859	-3.5892742869
C	-4.3895915869	0.1542766719	-0.9862133482
H	0.0403251589	-0.2031964399	-3.2569741735
H	-1.3288711085	-1.1830964094	-0.3063589418
H	2.9940890322	-1.3346058241	-0.3205079299
H	-2.3253377812	2.7587310777	-1.7592762800
H	1.1467960557	-1.6326652054	-4.9465864671
H	-3.7371489361	-1.7781900714	-0.2606399224
H	4.1178156983	-2.7855557980	-2.0250810912
H	-4.7516049822	2.1642346030	-1.7147360781
H	3.1944814050	-2.9239461244	-4.3349992847
H	-5.4489445788	-0.1142100709	-0.9721310650
C	3.9607062490	1.3669997119	-3.7622596706
C	3.1332534838	1.8445256473	-4.9538298935
C	1.8785057788	2.6164989473	-4.5260340807
C	1.2431210998	3.2726310891	-5.7445080725
N	-0.1532786767	3.9051846094	-5.5992304508
C	-0.3300965446	4.4891362398	-4.2045799791
C	-1.7498161033	4.8227807326	-3.7596268066
C	-1.7182919192	5.4584070274	-2.3644974070
C	-3.1182253655	5.7399253551	-1.8208454693
C	-0.1775896442	4.9921794187	-6.6743247285
C	-1.4651146121	5.7738211328	-6.9036050314
C	-1.3694075038	6.5943541204	-8.2017274574
C	-1.4278556530	5.7592426105	-9.4824398364
C	-1.2212067479	2.8812061149	-5.9278473247
C	-1.2327307337	1.6237371536	-5.0714809319
C	-2.5072012140	0.8147080551	-5.3366909494
C	-2.5389067788	-0.5107170602	-4.5782660188
H	4.8310729542	0.7777097709	-4.0912602655
H	3.3615578803	0.7350200013	-3.0905911228
H	4.3334247807	2.2210469266	-3.1723503718
H	3.7553749823	2.4848324342	-5.6045985613

H	2.8292526564	0.9811742170	-5.5715705102
H	2.1621179196	3.3857859534	-3.7913725380
H	1.1919097178	1.9315016598	-4.0140473546
H	1.1464920324	2.5566625748	-6.5721720358
H	1.9030681523	4.0802069451	-6.0846167528
H	0.3158569705	5.3776748021	-4.1718994618
H	0.0737215987	3.7567243369	-3.5004352659
H	-2.3579800748	3.9057141012	-3.7171385103
H	-2.2574923289	5.5055548463	-4.4522496876
H	-1.1719405222	4.7919364501	-1.6747239969
H	-1.1376535088	6.3965083245	-2.4063278630
H	-3.7069500034	4.8113171270	-1.7337167163
H	-3.0738000125	6.2033978014	-0.8226839466
H	-3.6723584542	6.4223151766	-2.4866852110
H	0.6312668220	5.6840469495	-6.4067882256
H	0.1176383743	4.4703345704	-7.5938446269
H	-2.3385331447	5.1073694586	-6.9713606664
H	-1.6406067914	6.4609235857	-6.0646979597
H	-0.4434276964	7.1967905886	-8.1858906408
H	-2.2016212905	7.3173674378	-8.2029019591
H	-0.5858223051	5.0522108651	-9.5589778478
H	-2.3606334066	5.1722278100	-9.5276445412
H	-1.3933788800	6.4049589736	-10.3742313357
H	-2.1843071532	3.3948605016	-5.8485684522
H	-1.0714870619	2.6229668403	-6.9853921195
H	-0.3531948549	1.0020626456	-5.2976404059
H	-1.1845493300	1.8771937506	-4.0022432271
H	-3.3823984597	1.4264140555	-5.0545018467
H	-2.5990959142	0.6267105729	-6.4212362171
H	-3.4697932072	-1.0633850711	-4.7809483458
H	-1.6937669721	-1.1566091617	-4.8687702700
H	-2.4766510312	-0.3480585625	-3.4913731439

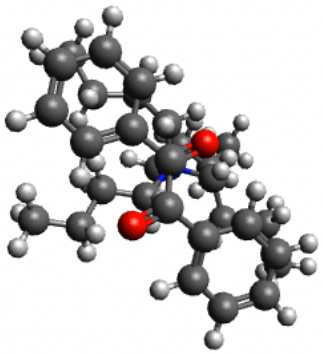

Figure S52. Benzil radical anion with TBA^+

Benzil radical anion with TBA^+

H	-5.0457452780	-1.2231545882	-0.1586186717
C	-4.5139965029	-0.4280540342	-0.6894265726
C	-5.2296737189	0.4985904887	-1.4561423872
H	-6.3186650933	0.4354804953	-1.5288991049
C	-3.1214884314	-0.3550141153	-0.5924257043
C	-4.5304249124	1.5086091478	-2.1290812097
H	-2.5711579891	-1.0727459321	0.0091641633
C	-2.3977842566	0.6454634780	-1.2801091296
C	-3.1405961708	1.5752587771	-2.0445616736
H	-5.0735377460	2.2432403107	-2.7305899037
O	-0.4938227597	-0.8587646029	0.3768162704
C	-0.0391909535	-0.0617827637	-0.4940448855
C	-0.9029636782	0.7659137705	-1.3389131274
H	-2.5890300517	2.3472139226	-2.5826294602
H	1.5883795272	-1.9909040080	0.2237491097
C	2.1572019767	-1.1940039954	-0.2579592909
C	1.4490533341	-0.0610354604	-0.7158864398
O	-0.4216199435	1.5613433063	-2.2069830924
C	3.5392828448	-1.3007101828	-0.4112900829
C	2.1934961488	0.9769060707	-1.3166812732
H	4.0579447725	-2.1970054727	-0.0590146422
C	4.2631091379	-0.2610945351	-1.0092307851
H	1.6692977147	1.8598129856	-1.6724135565
C	3.5812451326	0.8775950789	-1.4513515689
H	5.3474107705	-0.3363688359	-1.1248659533
H	4.1363330921	1.7004729714	-1.9104752015
N	-0.2916721415	-1.1569856472	-4.7786831575
C	1.0080350553	-0.3528362206	-4.7974590677
C	-0.2026999426	-1.5255197283	-7.3374182724
C	-0.3827136734	-2.1267001056	-5.9388157567
H	-1.3648324211	-2.6003260491	-5.8455245861
H	0.3651385252	-2.9084042559	-5.7524459184
C	2.2960775100	-1.1318491710	-4.5699494986
H	0.8789238877	0.4094407801	-4.0156340434
H	1.0315919074	0.1613116882	-5.7655962158
C	3.5098090501	-0.2653765725	-4.9222033896
H	2.3207100257	-2.0493394083	-5.1801207439
H	2.3760243685	-1.4414527618	-3.5170518443
C	4.8318832876	-0.9876289076	-4.6728296117
H	3.4729266363	0.6632024517	-4.3278270842
H	3.4448130217	0.0420555549	-5.9811126112

H	4.9277070544	-1.2755935759	-3.6136902838
H	5.6922484487	-0.3484147590	-4.9275701476
H	4.9021314316	-1.9064158313	-5.2790503863
C	1.1963251767	-1.6665363485	-7.9479403449
H	-0.5104844212	-0.4681092213	-7.3538498875
H	-0.9188177540	-2.0429725866	-7.9970185122
C	1.2552066127	-1.1342195589	-9.3785758968
H	1.4878913291	-2.7314387241	-7.9294459630
H	1.9424539966	-1.1369169518	-7.3351518994
H	2.2626372046	-1.2501493723	-9.8086924938
H	0.9964871782	-0.0623683642	-9.4124682207
H	0.5444911370	-1.6674718849	-10.0322718798
C	-1.4034851008	-0.0899768463	-4.8378031219
C	-2.7600734709	-0.3800883067	-5.4834141809
H	-0.9540919400	0.7240713971	-5.4167154189
H	-1.5062761201	0.2885981325	-3.8159981181
C	-3.8425010851	-1.1622373047	-4.7350674571
H	-2.6330341205	-0.7919207547	-6.4964084219
H	-3.1551997842	0.6387321223	-5.6461347204
C	-5.2164030828	-0.9647077631	-5.3760716895
H	-3.6063942807	-2.2361007129	-4.7172162395
H	-3.8798571146	-0.8261327284	-3.6872158465
H	-5.2170101015	-1.2869369664	-6.4312952776
H	-5.5155540835	0.0968276144	-5.3518138540
H	-5.9897422314	-1.5441193005	-4.8469911501
C	-0.2806208121	-1.9398313401	-3.4738532962
C	-1.5451541940	-2.6642720170	-3.0599950817
H	0.0013854260	-1.2178209867	-2.7004548802
H	0.5385752982	-2.6612623472	-3.5720586566
C	-1.2861549550	-3.4951055739	-1.7977627544
H	-2.3364178982	-1.9384591073	-2.8398860671
H	-1.9066268262	-3.3265845329	-3.8617679574
C	-2.5519712747	-4.1910927162	-1.2995379025
H	-0.8930785300	-2.8344104707	-1.0075109142
H	-0.4999680894	-4.2429517631	-2.0054108912
H	-3.3335486643	-3.4530018812	-1.0546178125
H	-2.3537977570	-4.7851390782	-0.3930381844
H	-2.9646886638	-4.8700435128	-2.0648182142

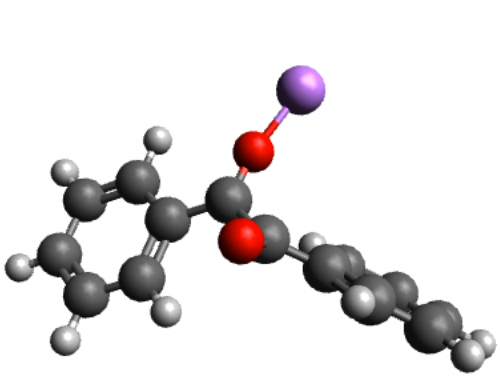

Figure S53. Benzil neutral with Li^+

Benzil neutral with Li^+

O	0.3856060680	1.4606492908	1.5319618707
O	-0.5241915862	1.4386367544	-1.5100762426
C	1.7953241020	0.1724514809	0.0919019445
C	-1.9011726346	0.1428274067	-0.0766329774
C	0.5376344991	0.8236795139	0.5041614007
C	-0.6570572859	0.8003705350	-0.4586553916
C	1.8622694048	-0.6439476396	-1.0528860634
C	-1.9785277354	-0.6423360137	1.0938075863
C	2.9404616290	0.3580927508	0.8892930902
C	-3.0296829721	0.2691393708	-0.9153590442
C	3.0653962724	-1.2617982817	-1.3962692193
C	-3.1705464506	-1.2867714884	1.4171396170
C	4.1397334371	-0.2559026344	0.5389791000
C	-4.2170151102	-0.3731278348	-0.5828087756
C	4.2025224266	-1.0655770866	-0.6043758573
C	-4.2871376861	-1.1507256914	0.5830334695
H	0.9790778314	-0.8053471477	-1.6747991237
H	-1.1114146571	-0.7488636679	1.7475811273
H	2.8683902881	0.9895105950	1.7770686820
H	-2.9554968659	0.8755067157	-1.8198746320

H	3.1168899164	-1.8972470320	-2.2832439638
H	-3.2325171587	-1.8962836241	2.3211787846
H	5.0303082553	-0.1075959791	1.1542227697
H	-5.0929710414	-0.2732527252	-1.2276157162
H	5.1445064035	-1.5477739538	-0.8777145450
H	-5.2212026563	-1.6558063450	0.8419243441
Li	0.0149580727	2.3798730908	-2.8858829481

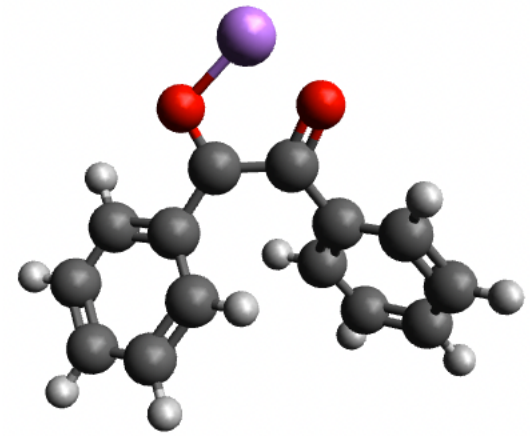

Figure S54. Benzil radical anion with Li^+

Benzil radical anion with Li^+

O	1.1654945232	2.7669790195	0.5473365415
O	-1.4083362038	2.7420966728	0.0552693884
C	1.5173575369	0.4494375144	0.1465790411
C	-1.6456239348	0.3770709332	0.0960666466
C	0.6301018044	1.6282737515	0.2978695738
C	-0.8170950080	1.6069829192	0.1310481774
C	1.2601217552	-0.5881076140	-0.7721263639
C	-1.3703847038	-0.7427586934	0.9049457515
C	2.7108911461	0.4045770672	0.8945749729
C	-2.7962983765	0.3563030273	-0.7162248223
C	2.1530132653	-1.6520750167	-0.9106730109

C	-2.2069200679	-1.8598017502	0.8793223469
C	3.5979425279	-0.6642735108	0.7613877036
C	-3.6247876342	-0.7663692496	-0.7503002790
C	3.3202992953	-1.7004709301	-0.1387524314
C	-3.3319346183	-1.8805286939	0.0459147096
H	0.3638172035	-0.5547092876	-1.3927881835
H	-0.5040882157	-0.7320110923	1.5683717257
H	2.9266481375	1.2206707788	1.5870353434
H	-3.0246149402	1.2315992867	-1.3280671775
H	1.9395773510	-2.4458467753	-1.6314294604
H	-1.9829596931	-2.7174615857	1.5190768523
H	4.5122123310	-0.6896286683	1.3603831655
H	-4.5047706812	-0.7733952261	-1.3991145265
H	4.0153757924	-2.5373313345	-0.2455418813
H	-3.9826564184	-2.7585458050	0.0237215402
Li	-0.1476521741	4.0383042630	0.3747646561

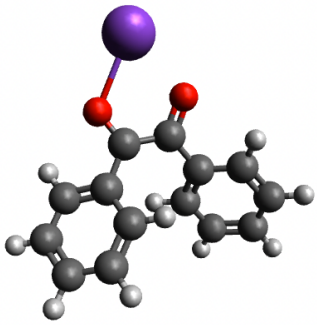

Figure S55. Benzil radical anion with K^+

Benzil radical anion with K^+

O	1.1973887899	2.7582996765	0.5912766593
O	-1.4454631513	2.7334142379	-0.0203443960
C	1.4880013342	0.4444090736	0.1347776818
C	-1.6121106750	0.3685110208	0.0971807922
C	0.6295784340	1.6545036559	0.3051723649
C	-0.8180248952	1.6322243873	0.1058359168
C	1.2351212676	-0.5446784764	-0.8375893482

C	-1.3234666253	-0.7192110481	0.9451054022
C	2.6490634817	0.3186531910	0.9234835724
C	-2.7482351021	0.2851843916	-0.7314557062
C	2.0903963449	-1.6382581115	-0.9861858454
C	-2.1234673645	-1.8635229863	0.9375271114
C	3.4994748559	-0.7796860519	0.7821707607
C	-3.5417321397	-0.8634841189	-0.7481493745
C	3.2214003507	-1.7677534776	-0.1705009583
C	-3.2308481062	-1.9459520283	0.0842707139
H	0.3647592393	-0.4521739649	-1.4891964967
H	-0.4698905582	-0.6638580873	1.6230303101
H	2.8683255870	1.0961529570	1.6583911270
H	-2.9923457963	1.1362613902	-1.3711557248
H	1.8759610350	-2.3924745193	-1.7484189480
H	-1.8845208069	-2.6945775623	1.6068382596
H	4.3854961207	-0.8668665182	1.4173773465
H	-4.4086701874	-0.9161531910	-1.4127410050
H	3.8867085923	-2.6278963394	-0.2834776681
H	-3.8530761441	-2.8447450024	0.0753691859
K	-0.1750938812	4.9126575021	0.4200582660

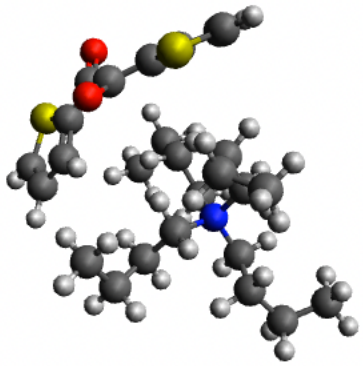

Figure S56. 2,2'-thenil neutral with TBA^+

2,2'-thenil neutral with TBA^+

S	0.6329354786	-4.0114820803	2.3310208771
S	-4.6930168093	-0.4532231326	-0.1752727485
O	-2.1369069517	-4.0583530603	1.1876254971
O	-2.6285306062	-0.7935082429	1.9754544916
C	-0.3693843229	-2.6547614828	1.8723972958
C	-3.5319300532	-1.7457467897	0.0161326017
C	-1.7142280932	-2.9265941373	1.3839994399
C	-2.6408296015	-1.7119823644	1.1668345884
C	0.3254994055	-1.4573893270	1.9820265421

C	-3.5957951587	-2.6399157989	-1.0438368950
C	1.6605987899	-1.6397529741	2.4230766018
C	-4.5743581790	-2.2796822575	-2.0045306550
C	1.9607668498	-2.9673186008	2.6547411743
C	-5.2504444277	-1.1271235995	-1.6571943559
H	-0.1167727668	-0.4906434506	1.7448956878
H	-2.9583172995	-3.5195686485	-1.1113555204
H	2.3733583507	-0.8268675061	2.5685285594
H	-4.7794125378	-2.8468971858	-2.9133121677
H	2.9041420384	-3.3845801305	3.0080754428
H	-6.0508053040	-0.6330324987	-2.2087131795
C	-2.0035438158	0.7646894630	-2.4854339926
C	-0.8849962994	0.4345836775	-1.4954723404
C	-0.2667904715	-0.9614498928	-1.6672595220
C	0.3739296200	-1.1223690090	-3.0351320913
N	0.9686184893	-2.4861448740	-3.3484030515
C	-0.0982773471	-3.5592517868	-3.3725709744
C	-1.2653572660	-3.3010104721	-4.3218209771
C	-1.9769314301	-4.6101919862	-4.6974832566
C	-2.5065899117	-5.4271142017	-3.5174571735
C	2.0818294140	-2.8212732691	-2.3443078469
C	1.7152617638	-3.5781622026	-1.0664473295
C	1.7210725616	-5.1133929075	-1.1286724601
C	3.0607194793	-5.7230225387	-1.5422765584
C	1.6326224256	-2.3369703811	-4.7142349850
C	2.0337852235	-3.6328280152	-5.4068955965
C	2.9263845458	-3.3549165130	-6.6268656951
C	4.3315560679	-2.8594152001	-6.2795496482
H	-2.4768937943	1.7270066769	-2.2352019612
H	-1.6333493354	0.8424355192	-3.5202024381
H	-2.7891262423	-0.0061864565	-2.4673253070
H	-0.0867573510	1.1949642645	-1.5641128989
H	-1.2786442514	0.4966318960	-0.4676097976
H	-1.0507545607	-1.7186140610	-1.5195777823
H	0.4816890196	-1.1099580330	-0.8768929746
H	-0.3522231480	-0.9256665008	-3.8311635715
H	1.1989671993	-0.4070365928	-3.1578146524
H	0.4177115776	-4.4888854139	-3.6355825586
H	-0.4628251108	-3.6657203478	-2.3472652383
H	-1.9799602429	-2.6057336800	-3.8527154847
H	-0.9203711138	-2.8217526723	-5.2503288463
H	-1.2778795776	-5.2311836173	-5.2857596248
H	-2.8101598513	-4.3612604274	-5.3755793178
H	-3.2232431269	-4.8489458282	-2.9135852059

H	-3.0258098990	-6.3314037527	-3.8720793744
H	-1.6967155346	-5.7564747690	-2.8458549272
H	2.5275959900	-1.8494439480	-2.0999162545
H	2.8354284442	-3.3870109174	-2.9017753078
H	0.7648782480	-3.2240985437	-0.6477004995
H	2.4768749410	-3.2699767871	-0.3307245728
H	1.4573072457	-5.4717561322	-0.1204462747
H	0.9246841145	-5.4861542980	-1.7918578359
H	3.3273660424	-5.4763409808	-2.5830268404
H	3.8780434720	-5.3637486747	-0.8942610648
H	3.0301393703	-6.8216024123	-1.4681662790
H	0.9379036073	-1.7730147608	-5.3477326659
H	2.5022085631	-1.6930900467	-4.5316772764
H	1.1335354190	-4.1721275818	-5.7371557157
H	2.5709182665	-4.3040319292	-4.7169155246
H	2.4226621186	-2.6281221563	-7.2889677204
H	3.0046820873	-4.2898977990	-7.2056722738
H	4.8504993014	-3.5770362989	-5.6218994269
H	4.3155589256	-1.8859782185	-5.7629308520
H	4.9404433860	-2.7351710216	-7.1890952120

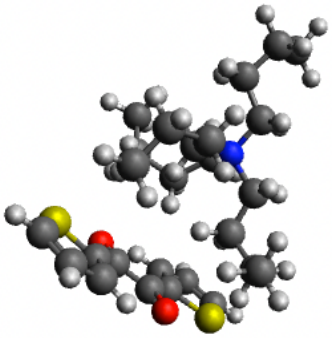

Figure S57. 2,2'-thenil radical anion with TBA^+

2,2'-thenil radical anion with TBA^+

S	0.4653422339	0.7183129275	1.5450882405
S	-3.5402157368	-4.5872845714	0.0576476476
O	-2.0008977806	-0.2502068404	0.4382986439
O	-1.2663715681	-3.5632752965	1.4793040337
C	-0.0953290603	-0.9469692950	1.6279805805
C	-3.0932907085	-2.8882517060	0.1601894307
C	-1.3791751418	-1.2185519693	0.9665547979
C	-1.8655491698	-2.6001149225	0.9160238104

C	0.8242999467	-1.7309025693	2.3116622460
C	-4.0367054835	-2.1025815971	-0.4887294583
C	1.9638580095	-0.9995014414	2.7577874615
C	-5.1068291188	-2.8592712110	-1.0499085010
C	1.9131609563	0.3332867554	2.4180343072
C	-4.9774332511	-4.2119091676	-0.8379647655
H	0.6556896735	-2.7920353640	2.4726882526
H	-3.9420402925	-1.0207335368	-0.5288536843
H	2.7921434876	-1.4462986945	3.3124643431
H	-5.9413004824	-2.4149405019	-1.5969919930
H	2.6471310051	1.1098228772	2.6335201408
H	-5.6426775215	-5.0101552177	-1.1665191621
C	-1.4605790127	0.9224673739	-3.3304015663
C	-0.3855541357	0.7097388714	-2.2631502425
C	0.0480930343	-0.7540006780	-2.0995148121
C	0.9001127152	-1.2120767968	-3.2739919281
N	1.1447976594	-2.7096959907	-3.4034320922
C	-0.1540948401	-3.4544736731	-3.6115651111
C	-0.9670384492	-3.0324149229	-4.8287144247
C	-2.1993520070	-3.9329772028	-4.9988722582
C	-3.2221557773	-3.8053208745	-3.8701160724
C	1.8934121399	-3.2348838587	-2.1709779191
C	1.0889203063	-3.6631976484	-0.9424714288
C	0.5239708485	-5.0917593865	-0.8997871508
C	1.5625805897	-6.1932810699	-1.1115600507
C	2.0729471977	-2.8718651353	-4.6021890107
C	2.2556880623	-4.2914239689	-5.1242659413
C	3.3350623467	-4.3483312932	-6.2169941422
C	4.7597787329	-4.1027217747	-5.7165934670
H	-1.7647984461	1.9802774774	-3.3818990498
H	-1.1189626348	0.6320298952	-4.3378838233
H	-2.3586952081	0.3247247383	-3.0993167185
H	0.4985299496	1.3365378686	-2.4794731970
H	-0.7757901342	1.0326920574	-1.2871816540
H	-0.8566659365	-1.3702078855	-1.9949535200
H	0.6108773741	-0.8545868238	-1.1620135760
H	0.4507092675	-0.9063521894	-4.2248183208
H	1.8974201346	-0.7546342602	-3.2239278369
H	0.1061762905	-4.5169785354	-3.6745609536
H	-0.7382707482	-3.3128606982	-2.6993284230
H	-1.3015548031	-1.9885383712	-4.7238300775
H	-0.3564143753	-3.0857232950	-5.7426217909
H	-1.8690115399	-4.9829857155	-5.0942334703
H	-2.6777070465	-3.6746991873	-5.9583389118

H	-3.5589297982	-2.7618374655	-3.7577523958
H	-4.1117383727	-4.4239076575	-4.0655772663
H	-2.8174205905	-4.1211640423	-2.8961299712
H	2.5811068922	-2.4214222040	-1.9081452814
H	2.5054848207	-4.0725799588	-2.5207708874
H	0.2962521345	-2.9450043372	-0.7066217264
H	1.8053107140	-3.5671292411	-0.1088408363
H	0.0550846179	-5.1984583118	0.0904227832
H	-0.2994599825	-5.2156146546	-1.6203335636
H	1.9789275399	-6.1827011809	-2.1324754670
H	2.4059569258	-6.0865862183	-0.4081021988
H	1.1174835153	-7.1887562134	-0.9542702050
H	1.6746838953	-2.2299955790	-5.3977124746
H	3.0286797796	-2.4383650156	-4.2806302638
H	1.3093082432	-4.6616665333	-5.5452102176
H	2.5340662650	-4.9822952495	-4.3121960109
H	3.0856424284	-3.6241331177	-7.0131287312
H	3.2823952464	-5.3449153557	-6.6855903776
H	5.0273567550	-4.8194781136	-4.9220464069
H	4.8896436718	-3.0875626480	-5.3078322796
H	5.4881677477	-4.2203906060	-6.5346186519

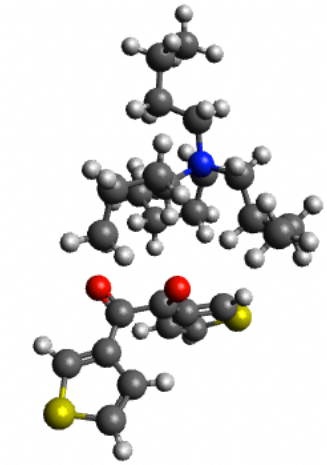

Figure S58. 3,3'-thenil neutral with TBA^+

3,3'-thenil neutral with TBA^+

C	-0.1776067475	-0.5456543913	0.8570532325
C	-4.7179200561	-4.4710771290	1.1315032292
O	-1.8867991860	-1.7822999076	-1.1447294758
O	-2.0339531721	-4.6189233395	0.0368088905
C	-0.8908003206	-1.7237035087	1.0171776713
C	-3.9052282707	-3.3860231625	0.8424835977

C	-1.7704236915	-2.2597157986	-0.0238489045
C	-2.5539862709	-3.5432687369	0.2960045148
C	-0.6389197147	-2.3470555913	2.2896299033
C	-4.5389317498	-2.1301129680	1.1469141491
C	0.2579167464	-1.6424434780	3.0454078121
C	-5.8001636750	-2.2937799095	1.6520145215
S	0.7963356398	-0.2083402901	2.2223913117
S	-6.2292920190	-3.9749148644	1.7627224089
C	-1.1290251219	1.0949112245	-4.3869639152
C	0.1364133958	1.1538378378	-3.5284437146
C	0.5933349592	-0.2143337693	-2.9953843072
C	1.1934504031	-1.0565382481	-4.1123154313
N	1.4550538455	-2.5253141686	-3.8129141831
C	0.1583925420	-3.2757227669	-3.5861036164
C	-0.8349238762	-3.2061621271	-4.7441090451
C	-1.9112066427	-4.2957854569	-4.6360171538
C	-2.8012121740	-4.1892785369	-3.3982727301
C	2.4069112106	-2.6687045390	-2.6191757753
C	1.8242808246	-2.6635192093	-1.2041906386
C	1.3631990408	-4.0026220915	-0.6088627515
C	2.4249781369	-5.1025385000	-0.6096121846
C	2.1981979018	-3.0638571090	-5.0330439111
C	2.3135340549	-4.5796854646	-5.1315420397
C	3.2751954110	-4.9892618046	-6.2582933860
C	4.7467185572	-4.6785258530	-5.9774586085
H	-1.4320951996	2.1018458082	-4.7152620896
H	-0.9882231283	0.4836575259	-5.2931892520
H	-1.9672823539	0.6575440286	-3.8192063039
H	0.9586412843	1.6240586369	-4.0971973743
H	-0.0458795977	1.8084053694	-2.6600955682
H	-0.2720912713	-0.7077583998	-2.5287009568
H	1.3424704366	-0.0575910774	-2.2053593309
H	0.5477386049	-1.0478815300	-4.9971601117
H	2.1652416230	-0.6422562258	-4.4136333551
H	0.4406339169	-4.3141016083	-3.3767421081
H	-0.2917448439	-2.8654762703	-2.6784363635
H	-1.3186448744	-2.2162219803	-4.7641051087
H	-0.3187920137	-3.3266110217	-5.7079826355
H	-1.4187734723	-5.2847052853	-4.6583766149
H	-2.5344744300	-4.2444584249	-5.5445013900
H	-3.2936073841	-3.2044714540	-3.3464857210
H	-3.5861058704	-4.9623512903	-3.4095262543
H	-2.2279933431	-4.3097883283	-2.4682707088
H	3.1166315563	-1.8407321457	-2.7394284917

H	2.9649851291	-3.5957996451	-2.7862985349
H	1.0212564047	-1.9245387852	-1.1137249010
H	2.6399322645	-2.2773291146	-0.5695822165
H	1.0597596782	-3.7969955188	0.4303492068
H	0.4506625447	-4.3657751125	-1.1037138396
H	2.6848247685	-5.4309588834	-1.6292477525
H	3.3542160418	-4.7623157161	-0.1215341815
H	2.0655036435	-5.9908799303	-0.0663240824
H	1.6863696964	-2.6681917390	-5.9184318817
H	3.1868700425	-2.5897935514	-4.9915326251
H	1.3243782337	-5.0181143200	-5.3306920185
H	2.6684810551	-5.0137988268	-4.1829031663
H	2.9601835196	-4.5036953234	-7.1992919491
H	3.1582024331	-6.0732119179	-6.4219312735
H	5.0828606085	-5.1702991564	-5.0491309763
H	4.9307566119	-3.5975550106	-5.8669160941
H	5.3874223723	-5.0365564330	-6.7988611683
H	-0.1896093327	0.1205190016	-0.0043075167
H	-1.0975176671	-3.2817663825	2.6153532138
H	0.6395366746	-1.8759409845	4.0388710593
H	-4.4780656665	-5.5250508758	0.9956960505
H	-4.0744140769	-1.1546987428	0.9942608328
H	-6.5095500673	-1.5292470898	1.9673722256

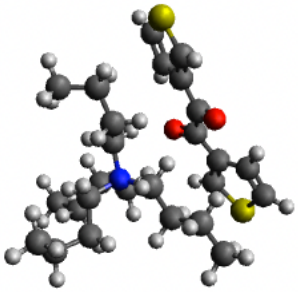

Figure S59. 3,3'-thenil radical anion with TBA^+

3,3'-thenil radical anion with TBA^+

S	-3.8318147718	1.5514386014	2.0345793227
S	0.8298590121	3.8128337309	-5.4076374697
O	-1.8341049649	0.9145590551	-1.9400650425
O	-2.0641691652	4.4290482072	-2.0085197486
C	-2.6783363342	2.2555017598	-0.1812834688
C	-0.6314101940	3.1258484010	-3.3729198280
C	-2.0027538231	2.0901248798	-1.4962884638
C	-1.5883295712	3.2728389752	-2.2480627064
C	-2.9190829547	3.4662756022	0.5676458615

C	0.1356361891	1.9616882498	-3.7514793696
C	-3.1271486866	1.1432594457	0.5125047863
C	-0.3361270003	4.2039488901	-4.1934853133
C	-3.5305331232	3.2432428446	1.7730456736
C	0.9624419568	2.1817657633	-4.8193657061
H	0.0471522717	1.0109681711	-3.2323652549
H	-3.0657505033	0.1088390403	0.1810178221
H	-0.7534413263	5.2064379878	-4.1275937206
H	-3.8264042904	3.9738625025	2.5257921376
H	1.6382290481	1.4793191084	-5.3067636432
H	-2.6433904886	4.4489580474	0.1931809903
C	-1.5338023652	0.8163269738	-7.1824515190
C	-2.5078561575	0.8113534229	-6.0062290167
C	-3.1444215672	2.1857770212	-5.7708263411
C	-4.0630177144	2.1170062976	-4.5564504971
N	-4.9211538921	3.3403892877	-4.2295859657
C	-5.2257711821	3.3190602541	-2.7311305633
C	-5.7015174539	1.9872338963	-2.1572079692
C	-6.2830234287	2.1864401267	-0.7492847548
C	-7.6573659392	2.8572744937	-0.7242504557
C	-6.2468402561	3.2949002900	-4.9598473710
C	-6.1960069503	3.2503351621	-6.4804032260
C	-7.5964740230	3.4271851393	-7.0863842647
C	-8.5857193532	2.3144294863	-6.7328311588
C	-4.1341845886	4.6117859535	-4.5268295810
C	-4.8175264548	5.9473654765	-4.2262818661
C	-5.6160398851	6.5901357690	-5.3661465543
C	-6.0865460803	7.9999604640	-5.0103701719
H	-1.0627186571	-0.1705871255	-7.3168292698
H	-2.0479635883	1.0760527475	-8.1232184392
H	-0.7319691949	1.5546932862	-7.0230638815
H	-3.3035545083	0.0651643145	-6.1811184844
H	-1.9840493805	0.4973275123	-5.0877678668
H	-3.6807747604	2.4941519315	-6.6788911985
H	-2.3446267844	2.9194555979	-5.5965876634
H	-3.4498128496	1.9267586665	-3.6684757700
H	-4.7668647687	1.2806293612	-4.6550948987
H	-4.3048909935	3.6454555008	-2.2300553565
H	-5.9888553771	4.0888113916	-2.5762653485
H	-4.8595675987	1.2837771542	-2.1004786815
H	-6.4700207116	1.5252339781	-2.7977583015
H	-6.3489354227	1.1988161297	-0.2656925803
H	-5.5675677624	2.7672550410	-0.1450258330
H	-8.0282971680	2.9549197178	0.3086506326

H	-7.6336226333	3.8702788060	-1.1587831200
H	-8.3972765597	2.2699137745	-1.2938226725
H	-6.7682369364	2.4122276193	-4.5745393368
H	-6.8078545507	4.1741151803	-4.6191531336
H	-5.5398168354	4.0426720841	-6.8700150111
H	-5.7802667978	2.2879692393	-6.8166689637
H	-7.4840090587	3.4799139948	-8.1820133831
H	-8.0050897395	4.4045894764	-6.7731227902
H	-9.5392800221	2.4525327113	-7.2667408007
H	-8.8153355693	2.2888319706	-5.6551699976
H	-8.1834791807	1.3255924071	-7.0114789667
H	-3.2325910837	4.5214982467	-3.9105775828
H	-3.8425341637	4.5694736628	-5.5806447488
H	-3.9936803496	6.6334810792	-3.9654521027
H	-5.4326864271	5.8904281493	-3.3148426839
H	-4.9827010715	6.6243375193	-6.2702019505
H	-6.4920491920	5.9774428535	-5.6311537199
H	-5.2316509668	8.6589182823	-4.7830838689
H	-6.7404909385	7.9867980098	-4.1219937013
H	-6.6532162053	8.4551092700	-5.8381168265

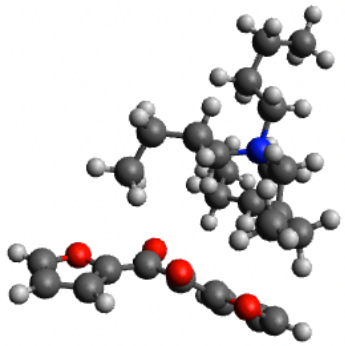

Figure S60. Furil neutral with TBA^+

Furil neutral with TBA^+

O	-0.5706791686	0.3174244427	0.4297968061
O	-4.2697653389	-4.5468913994	0.3988002419
O	-2.6887922040	-0.8497536190	-0.8790216161
O	-1.6340459154	-3.7893697189	0.5015777293
C	-0.9464879514	-0.9705099417	0.7064691579
C	-3.9092838554	-3.2362013870	0.2348761526
C	-2.0871810676	-1.4893371582	-0.0241376971
C	-2.4897942814	-2.9420708175	0.2822270810
C	-0.1019317059	-1.4927279805	1.6712448371

C	-5.0467756148	-2.4658565526	0.0725210806
C	0.8341137825	-0.4699735781	1.9850825784
C	-6.1511460280	-3.3587855341	0.1424009927
C	0.4970797927	0.6048709586	1.1961678310
C	-5.6128831495	-4.6090148197	0.3381890378
H	-0.1535757286	-2.4962036828	2.0835926124
H	-5.0690473405	-1.3911607650	-0.0856946557
H	1.6539707516	-0.5183554572	2.6987197118
H	-7.2078267851	-3.1138074369	0.0564488183
H	0.9173904236	1.6024201682	1.0844214608
H	-6.0564975583	-5.5967251415	0.4477680464
C	-0.9628592724	1.1698155260	-3.5396755485
C	0.3509079710	1.0367729509	-2.7672989978
C	0.7168589186	-0.4145498002	-2.4192603942
C	1.2509628437	-1.1487829872	-3.6392786896
N	1.4362965678	-2.6532535141	-3.5023382189
C	0.1116043422	-3.3491739956	-3.2730495060
C	-0.9487120733	-3.0738982806	-4.3347417809
C	-2.1155925573	-4.0669664103	-4.2426831203
C	-2.8444151020	-4.0584860360	-2.8989892028
C	2.4405844652	-2.9611928881	-2.3830743009
C	1.9268805895	-3.1296038107	-0.9505909710
C	1.4866005955	-4.5374309933	-0.5196611532
C	2.5634168387	-5.6116117107	-0.6741390482
C	2.0788862955	-3.1047976728	-4.8112469867
C	2.0951894666	-4.6065000370	-5.0650460440
C	2.9583608641	-4.9537504580	-6.2882987674
C	4.4609247548	-4.7567709582	-6.0790081844
H	-1.1882565260	2.2253159147	-3.7604773661
H	-0.9370883141	0.6315335236	-4.5015716756
H	-1.7961127557	0.7586649741	-2.9472007721
H	1.1785149752	1.5005769858	-3.3333063780
H	0.2703818071	1.5992309981	-1.8242118420
H	-0.1804891185	-0.9135587078	-2.0290416209
H	1.4692870292	-0.4198991067	-1.6176370311
H	0.5872163715	-1.0087503729	-4.4994400106
H	2.2374882654	-0.7557602849	-3.9196654590
H	0.3337337474	-4.4205528721	-3.2117833900
H	-0.2443079105	-3.0335837847	-2.2885644537
H	-1.3361240124	-2.0490973440	-4.2179359114
H	-0.5146362239	-3.1387254696	-5.3436255120
H	-1.7422715978	-5.0837005216	-4.4598419928
H	-2.8262325068	-3.8218155663	-5.0493844876
H	-3.1410301845	-3.0360792218	-2.6149174056

H	-3.7560767463	-4.6754073242	-2.9358711085
H	-2.2162669841	-4.4571781900	-2.0877906382
H	3.1631190200	-2.1378804671	-2.4364923645
H	2.9671486714	-3.8704452170	-2.6903465166
H	1.1381361710	-2.4051421080	-0.7145902719
H	2.7806831542	-2.8349848329	-0.3164573550
H	1.1865462473	-4.4685398067	0.5384407434
H	0.5749380281	-4.8434059335	-1.0549406509
H	2.8235739430	-5.7908857337	-1.7303102680
H	3.4903864395	-5.3279680562	-0.1472218566
H	2.2200876011	-6.5721158619	-0.2581925618
H	1.5458190632	-2.5928882143	-5.6214030878
H	3.0950922474	-2.6921421128	-4.7794819145
H	1.0703221282	-4.9662850421	-5.2397485242
H	2.4800248979	-5.1528123832	-4.1885303127
H	2.6163351590	-4.3597672440	-7.1547328699
H	2.7637224891	-6.0076202663	-6.5470008511
H	4.8213750425	-5.3558019635	-5.2258834303
H	4.7207618171	-3.7042628396	-5.8803973958
H	5.0256319997	-5.0691640506	-6.9717407490

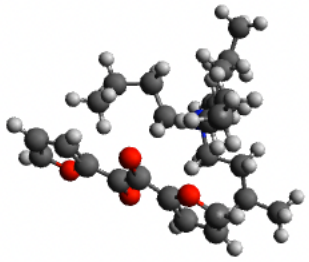

Figure S61. Furil radical anion with TBA^+

Furil radical anion with TBA^+

O	2.3631805918	3.7709202762	1.5405149353
O	-2.4663843122	1.1308806930	-1.0724334336
O	-0.0590027093	2.7003964444	2.0123741507
O	-0.2901658834	2.6428067366	-1.5270986996
C	1.5975055897	3.3849603332	0.4673906536
C	-1.7521242655	1.5929424535	0.0079711822
C	0.2895594819	2.8049455237	0.7990093737
C	-0.5523939264	2.3767694194	-0.3182737865
C	2.2941644844	3.6715263794	-0.6939709778
C	-2.3739172713	1.1581341738	1.1652394943
C	3.5319372556	4.2718202277	-0.2995168392
C	-3.5165372901	0.3968917722	0.7613509527

C	3.5180191302	4.3073711694	1.0693222988
C	-3.5212354312	0.4155457758	-0.6076312279
H	1.9313100032	3.4705462825	-1.6952069333
H	-2.0268136039	1.3778903418	2.1683664999
H	4.3280902308	4.6331765105	-0.9483353736
H	-4.2424860219	-0.0989978027	1.4040217651
H	4.2226257339	4.6637681108	1.8171431172
H	-4.1816243420	-0.0120198160	-1.3587055189
C	1.2993269516	5.9576074449	3.8575226324
C	0.4604181752	6.8916063110	2.9861923215
C	0.1616173810	6.3085063710	1.5994057303
C	-0.6158761981	7.3207646683	0.7724951582
N	-1.1014692494	6.8422249417	-0.5796087292
C	-2.0241905020	5.6410916559	-0.4431792431
C	-3.3332584989	5.8538975557	0.3003098488
C	-4.0716493523	4.5196688999	0.4867950112
C	-4.4715505117	3.8369868123	-0.8225662192
C	-1.7975298014	7.9755298015	-1.3361320972
C	-2.5887321935	8.9983326420	-0.5300186773
C	-3.3235233377	9.9473893097	-1.4838776756
C	-4.0887560764	11.0442769104	-0.7458013807
C	0.0514625003	6.3650670753	-1.4595916110
C	1.2809437792	7.2609539155	-1.4925149925
C	2.2028194807	6.8616761912	-2.6506958442
C	3.5312641181	7.6141379095	-2.6252739365
H	0.8367475109	4.9601509233	3.9285099414
H	2.3049720205	5.8162195760	3.4318083141
H	1.4132013116	6.3602376567	4.8766338986
H	-0.4968592010	7.1147732339	3.4904875657
H	0.9781103321	7.8611363463	2.8736310783
H	1.1045315933	6.0388658481	1.1031159745
H	-0.4047149577	5.3748163607	1.7277286462
H	-0.0095485636	8.2151787553	0.5834297809
H	-1.5048289837	7.6415116928	1.3247030039
H	-1.4334357450	4.8625918233	0.0518950687
H	-2.2065867104	5.3041677089	-1.4709106176
H	-3.9840280750	6.5480850683	-0.2537406892
H	-3.1459813252	6.2966461328	1.2905428097
H	-3.4407661410	3.8355064646	1.0791826272
H	-4.9732225200	4.7152914940	1.0909607554
H	-3.5934040768	3.4923234241	-1.3890800102
H	-5.0492986585	4.5213496987	-1.4672887341
H	-5.0914643065	2.9489227412	-0.6259660284
H	-2.4394739164	7.4766534061	-2.0751902565

H	-1.0108531905	8.5032758683	-1.8883988881
H	-3.3197395831	8.5171175557	0.1345717692
H	-1.9110886490	9.5865860256	0.1077823081
H	-4.0189130903	9.3627286434	-2.1118180369
H	-2.5941620784	10.4033123543	-2.1772025259
H	-4.6122837986	11.7097613811	-1.4505026106
H	-3.4079543487	11.6640649371	-0.1385361584
H	-4.8426232660	10.6134000049	-0.0657145343
H	0.3182128337	5.3560300117	-1.1248776097
H	-0.3828193288	6.2648653415	-2.4642553200
H	1.0026608869	8.3213488443	-1.6070648095
H	1.8338935138	7.1772062471	-0.5444227596
H	2.3902243515	5.7761205206	-2.6081247433
H	1.6806054567	7.0465431167	-3.6059205825
H	3.3727890207	8.7049846639	-2.6683944042
H	4.1682068462	7.3323044057	-3.4787479822
H	4.0904011275	7.3954628220	-1.7001130798

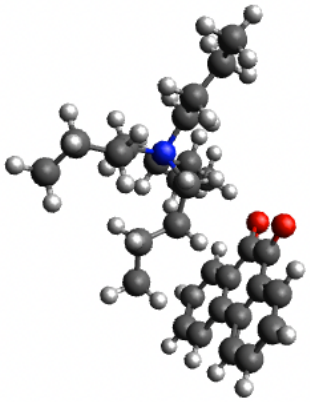

Figure S62. PQ neutral with TBA^+

PQ neutral with TBA^+

O	2.2278189382	3.3055173593	0.7840289392
O	-0.3039815564	3.7645941486	-0.0339297766
C	1.1358879766	-0.1239274308	0.2122905323
C	-0.2981941349	0.1211401433	-0.0753740876
C	2.0118533968	0.9543116531	0.4983536647
C	-0.8109177460	1.4429519451	-0.1352282351
C	1.5285080546	2.3473962251	0.5029979567
C	0.0623450861	2.6096522106	0.0938315177
C	1.6808349882	-1.4191113278	0.1956052227
C	-1.1933320869	-0.9332670839	-0.3238650631
C	3.3735199018	0.7236479555	0.7601580891

C	-2.1621948751	1.6783121562	-0.4396087940
C	3.0361451919	-1.6381134445	0.4475876385
C	-2.5360666313	-0.6906722491	-0.6202761452
C	3.8919031399	-0.5669309310	0.7323023948
C	-3.0299930317	0.6181060170	-0.6806813207
H	1.0514251267	-2.2796079989	-0.0274547218
H	-0.8515092331	-1.9669814131	-0.2900802962
H	4.0134851636	1.5791151620	0.9776381832
H	-2.5080755768	2.7126944814	-0.4811601519
H	3.4270914907	-2.6580622281	0.4184533394
H	-3.2028052713	-1.5358953913	-0.8075496974
H	4.9519403395	-0.7417743209	0.9285089815
H	-4.0807163189	0.8035418412	-0.9139696777
C	5.6432442598	3.8436604261	0.0831713504
C	5.3084620979	3.3826807767	-1.3337589218
C	4.1672096922	4.1926660938	-1.9607884715
C	3.9621893619	3.7714780597	-3.4098619565
N	2.6658651384	4.2238998806	-4.0722110020
C	1.4541114948	3.6082043542	-3.3803588823
C	1.5405659169	2.1416161766	-2.9672823533
C	1.6424264508	1.0466077613	-4.0328832505
C	1.6294733240	-0.3440004252	-3.3975681239
C	2.7949834537	3.8223389448	-5.5446887673
C	1.5174662612	3.6594098054	-6.3590249279
C	1.8451563152	3.3520178558	-7.8291725641
C	2.5252880817	2.0003371844	-8.0587519830
C	2.5973513833	5.7398224998	-3.9376441250
C	1.4607760702	6.4621666854	-4.6449916646
C	1.4494146987	7.9394704216	-4.2334084103
C	0.3493328674	8.7332385314	-4.9358011241
H	6.4365386847	3.2217156397	0.5276444146
H	4.7548042183	3.7820465456	0.7308369468
H	5.9908165855	4.8902456590	0.0890224137
H	6.2050671455	3.4538334806	-1.9751803062
H	5.0219022279	2.3162144559	-1.3237325682
H	4.4105160124	5.2650312544	-1.9039993122
H	3.2554675944	4.0418116443	-1.3638223133
H	4.7683441722	4.1686667711	-4.0415057376
H	3.9850031422	2.6794557982	-3.4998039991
H	0.5939833504	3.7835390709	-4.0335856291
H	1.2961142754	4.2093413038	-2.4762190513
H	0.6015196874	1.9760914051	-2.4144572560
H	2.3447499089	2.0047223721	-2.2285086594
H	0.8009279575	1.1377964478	-4.7392180995

H	2.5617107067	1.1612711013	-4.6290311758
H	2.4714837135	-0.4690157901	-2.6970586442
H	1.7040930397	-1.1335412554	-4.1615968439
H	0.7019379605	-0.5097481243	-2.8263176824
H	3.3568441652	2.8829490109	-5.5478016020
H	3.4425477528	4.5874339524	-5.9960260365
H	0.9062677557	2.8390120287	-5.9584324544
H	0.9022401140	4.5663181360	-6.3146326220
H	2.4710415010	4.1638009383	-8.2409894255
H	0.8982112928	3.3815283759	-8.3930513077
H	1.9200639053	1.1783617525	-7.6407536685
H	3.5218820616	1.9500250787	-7.5913155299
H	2.6588561577	1.8063008878	-9.1347750412
H	2.5393940078	5.9404510383	-2.8614233822
H	3.5659029305	6.1126725352	-4.2995333918
H	0.4871838590	6.0125491209	-4.3931895761
H	1.5808121319	6.3991140303	-5.7366871934
H	2.4343357073	8.3864224049	-4.4573830689
H	1.3219198891	8.0091619580	-3.1386584243
H	0.3586392648	9.7901780208	-4.6256911858
H	0.4739800715	8.7023038458	-6.0311593827
H	-0.6471310816	8.3220646830	-4.7024985791

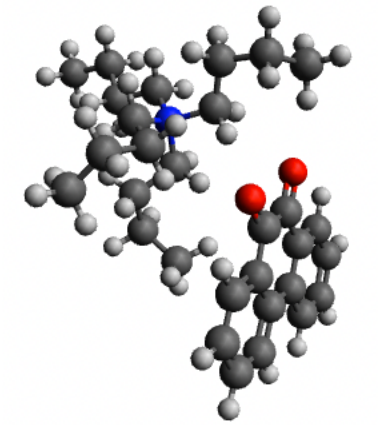

Figure S63. PQ radical anion with TBA^+

PQ radical anion with TBA^+

C	-1.2936971857	-2.2146783587	-3.0483214508
C	-0.4996872684	-2.6065549040	-1.8028618633
C	0.2293615994	-1.4406855112	-1.1192692598
C	-0.7541866296	-0.3883983877	-0.6134742701
N	-0.2201881514	0.6473038156	0.3791881744
C	-0.3193997361	0.1373604473	1.8069200659

C	0.3962249733	-1.1616455671	2.1449444627
C	0.3005666432	-1.4380981925	3.6501243724
C	0.9743834019	-2.7510456572	4.0455901766
C	1.2100281671	1.0402099435	0.0741159554
C	1.3978651392	1.8197624141	-1.2221372458
C	2.8783542484	1.9094870643	-1.6182794278
C	3.4770616886	0.5955536439	-2.1250249812
C	-1.1573231989	1.8452948134	0.2542894790
C	-0.8528092591	3.0330768121	1.1584079189
C	-1.6117043453	4.2836165913	0.6867355586
C	-3.1326495524	4.1195020210	0.6400015295
H	-0.6527940131	-1.7046063302	-3.7858009860
H	-2.1226336813	-1.5313712174	-2.8129513565
H	-1.7298474710	-3.1003779123	-3.5370198893
H	-1.1684372227	-3.0909199544	-1.0684410442
H	0.2576272306	-3.3619787487	-2.0719604252
H	0.8372447616	-1.8455666135	-0.3011580642
H	0.9275812967	-0.9821931011	-1.8362900079
H	-1.1490312703	0.1911100793	-1.4529021312
H	-1.6102582271	-0.8569555142	-0.1079103059
H	0.0675297980	0.9455262119	2.4398582768
H	-1.3948474286	0.0377155941	2.0096979692
H	-0.0547615232	-2.0051728119	1.6007835248
H	1.4584334242	-1.1135848386	1.8570068697
H	0.7594143231	-0.5993136916	4.2030305908
H	-0.7625928923	-1.4580593515	3.9491827385
H	2.0437440216	-2.7447347494	3.7753241447
H	0.9018601582	-2.9285043373	5.1303655708
H	0.5071784119	-3.6077072725	3.5315853999
H	1.5622025707	1.6304235434	0.9296609141
H	1.7924207991	0.1145689099	0.0682107190
H	0.8209508479	1.3683698181	-2.0434369859
H	0.9969730270	2.8366965607	-1.0990457058
H	3.4656398302	2.2845691762	-0.7605477000
H	2.9711035017	2.6748598157	-2.4067001258
H	3.4558906550	-0.1951558972	-1.3575672095
H	4.5279822193	0.7303863397	-2.4268661260
H	2.9196347572	0.2234643179	-3.0008799756
H	-2.1595882059	1.4444273117	0.4443904438
H	-1.1521336137	2.1346686974	-0.8040323169
H	-1.1285785392	2.8115454555	2.2024136460
H	0.2243380548	3.2601723150	1.1549021267
H	-1.2428205889	4.5660292253	-0.3156453282
H	-1.3455415315	5.1167116451	1.3590907168

H	-3.4333420014	3.3803839361	-0.1186049991
H	-3.6220518770	5.0755947332	0.3925347394
H	-3.5256004066	3.7860741390	1.6164644980
C	-1.4492267744	-0.3711218151	-7.2700255603
C	-0.5621074126	0.5579512613	-6.6947023866
C	-0.8674233292	1.1211032299	-5.4641482407
C	-2.0520264046	0.7799741617	-4.7722104665
C	-2.9558845693	-0.1556039809	-5.3532092034
C	-2.6225380898	-0.7142925462	-6.6069965304
C	-4.1763469704	-0.5222130264	-4.6293859514
C	-5.1142755898	-1.4461347190	-5.1425338582
C	-6.2602166339	-1.7912991392	-4.4342065810
C	-6.5090392258	-1.2163954675	-3.1738760328
C	-5.6036462517	-0.3058373958	-2.6493187751
C	-4.4333851962	0.0572809305	-3.3536308127
C	-3.5131090252	1.0216828395	-2.7254802974
O	-3.7595094994	1.5010747347	-1.5868501006
C	-2.2902306228	1.3879865073	-3.4549448620
O	-1.4434938213	2.1748899519	-2.9446426275
H	-1.2199851036	-0.8254352713	-8.2375047538
H	0.3602932953	0.8318694448	-7.2140634358
H	-0.1986362834	1.8428179321	-4.9918734206
H	-3.2912348628	-1.4383937321	-7.0743165401
H	-4.9455034299	-1.9071531464	-6.1166075908
H	-6.9648331753	-2.5104624671	-4.8599795605
H	-7.4086926727	-1.4862172297	-2.6140442047
H	-5.7658459002	0.1566598913	-1.6740158672

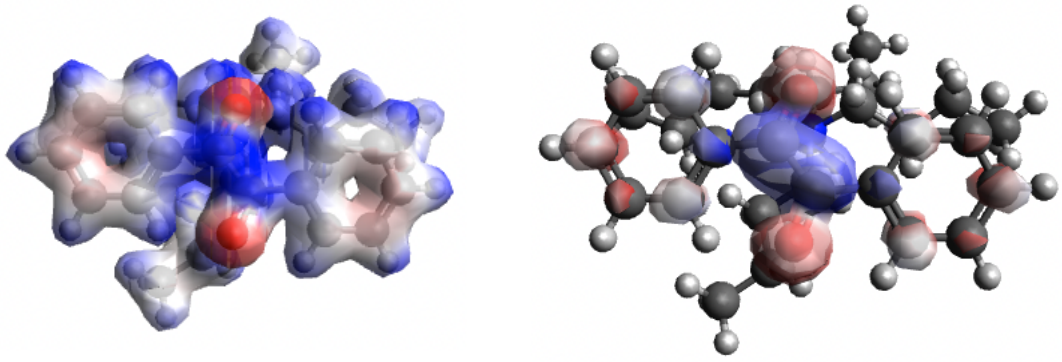

Figure S64. Electron (left) and spin (right) densities of benzil radical anions with TBA^+

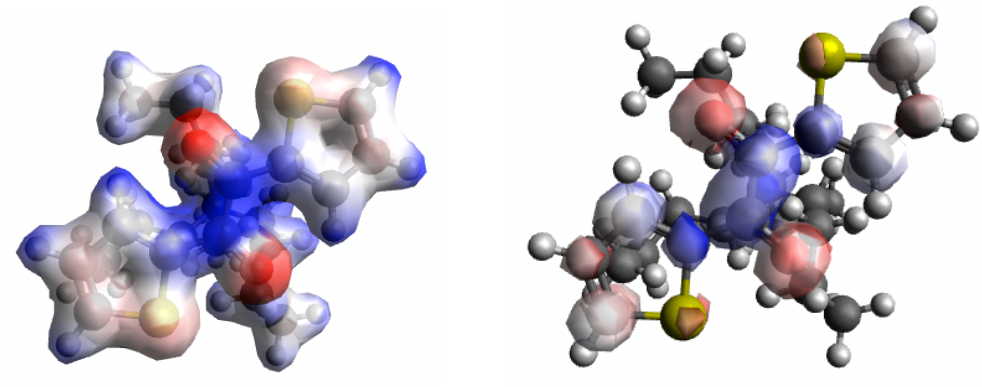

Figure S65. Electron (left) and spin (right) densities of 2,2'-thenil radical anion with TBA^+

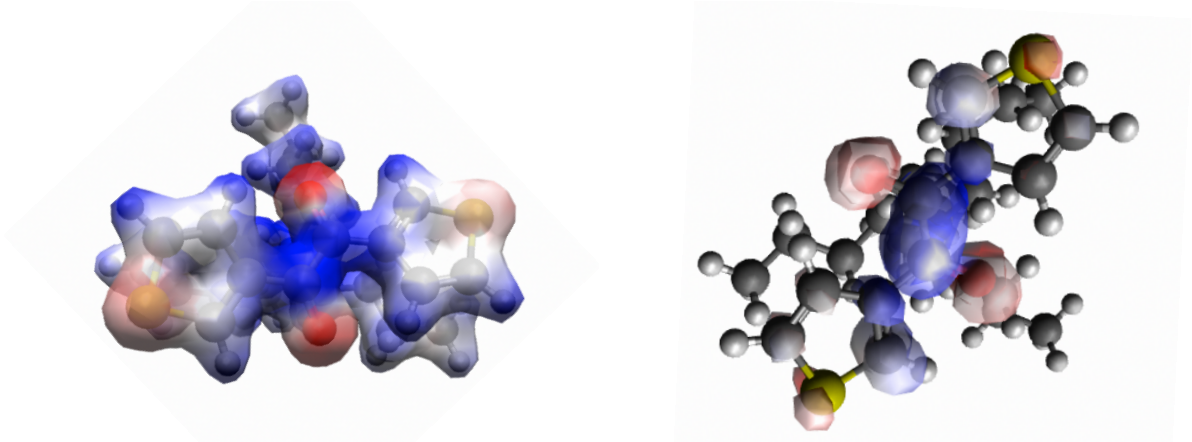

Figure S66. Electron (left) and spin (right) densities of 3,3'-thenil radical anion with TBA^+

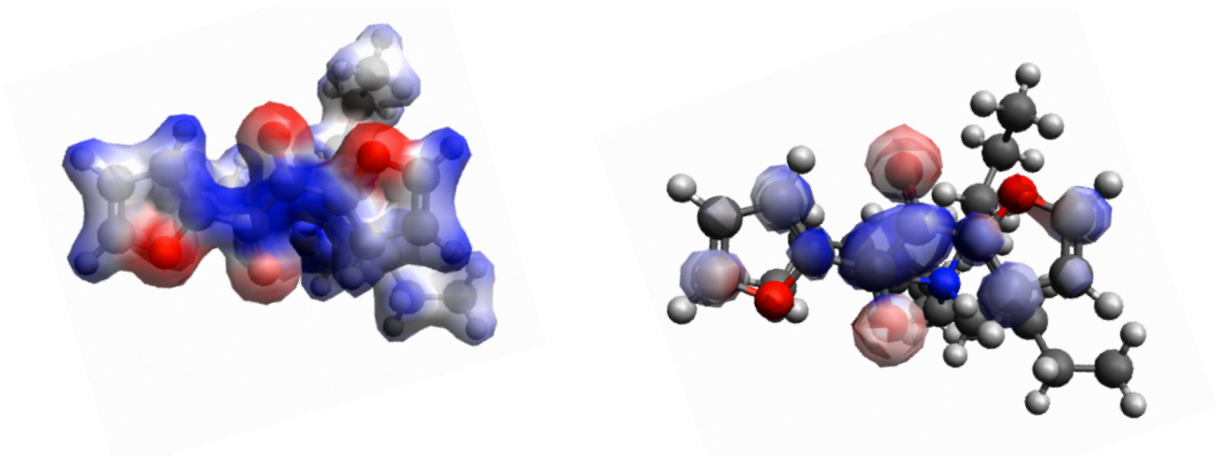

Figure S67. Electron (left) and spin (right) densities of furil radical anion with TBA^+

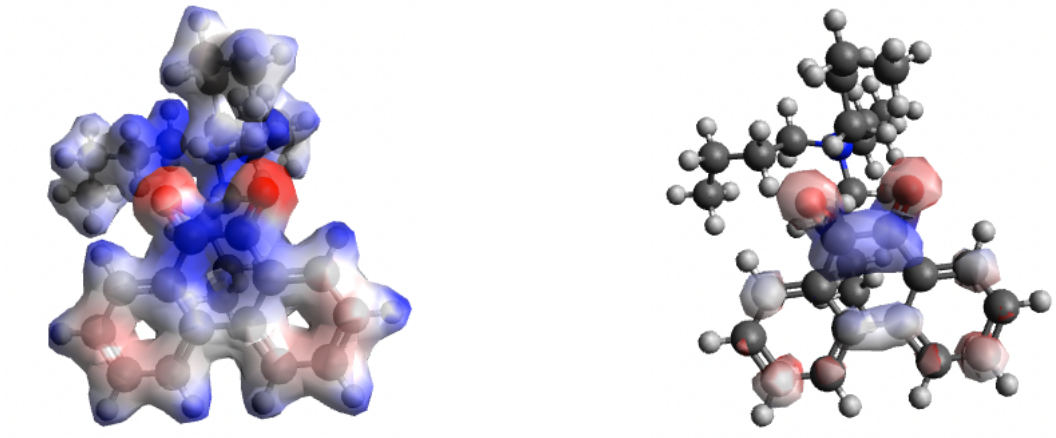

Figure S68. Electron (left) and spin (right) densities of PQ radical anion with TBA^+

Table S9. Mulliken charge and spin populations of benzil radical anion

0	O	:	-0.361065	0.269589
1	O	:	-0.361063	0.269588
2	C	:	0.001882	-0.044244
3	C	:	0.001884	-0.044243
4	C	:	0.049594	0.171413
5	C	:	0.049596	0.171418
6	C	:	-0.045174	0.052281
7	C	:	-0.045189	0.052280
8	C	:	-0.047787	0.058277
9	C	:	-0.047774	0.058276
10	C	:	0.004171	-0.028823
11	C	:	0.004174	-0.028822
12	C	:	0.005657	-0.030655
13	C	:	0.005664	-0.030654
14	C	:	-0.005518	0.060292
15	C	:	-0.005516	0.060291
16	H	:	-0.031383	-0.003591
17	H	:	-0.031393	-0.003591
18	H	:	-0.037278	-0.003717
19	H	:	-0.037276	-0.003717
20	H	:	-0.013125	0.001022
21	H	:	-0.013121	0.001022
22	H	:	-0.010747	0.001079
23	H	:	-0.010747	0.001079
24	H	:	-0.009233	-0.002926
25	H	:	-0.009231	-0.002925

Table S10. Mulliken charge and spin populations of PQ radical anion

0	O	-0.349479	0.254516
1	O	-0.349479	0.254517
2	C	0.096365	0.061019
3	C	0.096365	0.061019
4	C	-0.050000	-0.006548
5	C	-0.050002	-0.006548
6	C	0.011686	0.120626
7	C	0.011686	0.120626
8	C	-0.087169	-0.035427
9	C	-0.087166	-0.035427
10	C	-0.059650	0.056971
11	C	-0.059647	0.056970
12	C	0.004022	0.074438
13	C	0.004020	0.074438
14	C	0.013238	-0.020022
15	C	0.013233	-0.020022
16	H	-0.019107	0.001194
17	H	-0.019107	0.001194
18	H	-0.040633	-0.003590
19	H	-0.040632	-0.003590
20	H	-0.010018	-0.003664
21	H	-0.010019	-0.003664
22	H	-0.009253	0.000486
23	H	-0.009253	0.000486

References

1. Wang, H. *et al.* Redox Flow Batteries: How to Determine Electrochemical Kinetic Parameters. *ACS Nano* **14**, 2575–2584 (2020).
2. Lavagnini, I., Antiochia, R. & Magno, F. An Extended Method for the Practical Evaluation of the Standard Rate Constant from Cyclic Voltammetric Data. *Electroanalysis* **16**, 505–506 (2004).
3. Nicholson, R. S. Theory and Application of Cyclic Voltammetry for Measurement of Electrode Reaction Kinetics. *Anal. Chem.* **37**, 1351–1355 (1965).
4. Moutet, J., Mills, D., Hossain, M. M. & Gianetti, T. L. Increased performance of an all-organic redox flow battery model *via* nitration of the [4]helicenium DMQA ion electrolyte. *Mater. Adv.* **3**, 216–223 (2022).
5. Moutet, J., Veleta, J. M. & Gianetti, T. L. Symmetric, Robust, and High-Voltage Organic Redox Flow Battery Model Based on a Helical Carbenium Ion Electrolyte. *ACS Appl. Energy Mater.* **4**, 9–14 (2021).
6. Keil, P. & Jossen, A. Charging protocols for lithium-ion batteries and their impact on cycle life—An experimental study with different 18650 high-power cells. *Journal of Energy Storage* **6**, 125–141 (2016).
7. Stoll, S. & Schweiger, A. EasySpin, a comprehensive software package for spectral simulation and analysis in EPR. *Journal of Magnetic Resonance* **178**, 42–55 (2006).
8. Stoll, S. Computational Modeling and Least-Squares Fittingof EPR Spectra. in *Multifrequency Electron Paramagnetic Resonance* 69–138 (2014). doi:10.1002/9783527672431.ch3.
9. Hanuza, J. *et al.* Spontaneous and stimulated Raman scattering and infrared spectra of benzil ($C_{14}H_{10}O_2$) crystal: promoting modes of the stimulated effect, anharmonicity and scaling factors of fundamental vibrations. *J Raman Spectroscopy* **35**, 224–235 (2004).
10. Kolev, T. M. & Stamboliyska, B. A. Vibrational spectra and structure of benzil and its 18O- and d10-labelled derivatives: a quantum chemical and experimental study. *Spectrochimica Acta Part A: Molecular and Biomolecular Spectroscopy* **58**, 3127–3137 (2002).

11. Lopes, S., Gómez-Zavaglia, A., Lapinski, L., Chattopadhyay, N. & Fausto, R. Matrix-Isolation FTIR Spectroscopy of Benzil: Probing the Flexibility of the C−C Torsional Coordinate. *J. Phys. Chem. A* **108**, 8256–8263 (2004).
12. Mizuno, M., Iwata, K. & Takahashi, H. Time-resolved infrared and resonance Raman studies of benzil. Vibrational analysis and structures of the excited states. *Journal of Molecular Structure* **661–662**, 3–10 (2003).
13. Wilson, E. B. The Normal Modes and Frequencies of Vibration of the Regular Plane Hexagon Model of the Benzene Molecule. *Phys. Rev.* **45**, 706–714 (1934).
14. Ebihara, K., Hiura, H. & Takahashi, H. Time-resolved resonance Raman studies of the structures of the lowest triplet state and the radical anion of benzil. *J. Phys. Chem.* **96**, 9120–9127 (1992).
15. Locoge, N., Buntinx, G., Ratovelomanana, N. & Poizat, O. Time-resolved resonance Raman analysis of the lowest triplet (T1) state of benzil. *J. Phys. Chem.* **96**, 1106–1111 (1992).
16. Solin, S. A. & Ramdas, A. K. Raman Spectrum of Crystalline Benzil. *Phys. Rev.* **174**, 1069–1075 (1968).
17. Stoychev, G. L., Auer, A. A. & Neese, F. Automatic Generation of Auxiliary Basis Sets. *J. Chem. Theory Comput.* **13**, 554–562 (2017).
18. Weigend, F. & Ahlrichs, R. Balanced basis sets of split valence, triple zeta valence and quadruple zeta valence quality for H to Rn: Design and assessment of accuracy. *Phys. Chem. Chem. Phys.* **7**, 3297–3305 (2005).
19. Neese, F., Wennmohs, F., Becker, U. & Riplinger, C. The ORCA quantum chemistry program package. *The Journal of Chemical Physics* **152**, 224108 (2020).
20. Hanwell, M. D. *et al.* Avogadro: an advanced semantic chemical editor, visualization, and analysis platform. *Journal of Cheminformatics* **4**, 17 (2012).
21. Turney, J. M. *et al.* Psi4: an open-source ab initio electronic structure program. *WIREs Computational Molecular Science* **2**, 556–565 (2012).

22. Müller, M., Hansen, A. & Grimme, S. ωB97X-3c: A composite range-separated hybrid DFT method with a molecule-optimized polarized valence double-ζ basis set. *The Journal of Chemical Physics* **158**, 014103 (2023).